COO-2217-21

THE INVESTIGATION OF MOLECULAR MECHANISMS IN PHOTODYNAMIC ACTION AND RADIOBIOLOGY WITH NANOSECOND FLASH PHOTOLYSIS AND PULSE RADIOLYSIS

Progress Report

for Period July 1, 1976 - September 30, 1977

Leonard I. Grossweiner

Illinois Institute of Technology
Chicago, Illinois 60616

June 1977

Prepared For

THE U.S. ENERGY RESEARCH AND DEVELOPMENT ADMINISTRATION
UNDER CONTRACT NO. E(11-1)-2217

DISCLAIMER

The Investigation of Molecular Mechanisms in Photodynamic Action and Radiobiology with Nanosecond Flash Photolysis and Pulse Radiolysis

ABSTRACT

Laser flash photolysis investigations on aromatic amino acids and proteins have demonstrated that monophotonic electron ejection is the major initial act, leading to e^-_{aq} and the corresponding aromatic radicals, followed by back reactions limited by available e^-_{aq} scavengers. Results with ribonuclease A, lysozyme and carboxypeptidase A have led to information about the relationship of the photoionization efficiency of aromatic residues to the microenvironment. Measurements on the decay kinetics of photoelectrons have shown that the lifetimes and their dependence on scavenger concentrations and dose are inconsistent with homogeneous reactions. A new theory is proposed in which the photoelectron diffuses through the medium as a quasi-free particle, where original pair-recombination competes with scavenging and pair-pair interactions. This theory is in good agreement with laser flash photolysis studies on I^-, $Fe(CN)_6^{4-}$, tryptophan and tyrosine and consistent with earlier photochemical scavenging measurements. The general analysis of radiation sensitivity has been extended to suspensions of large biological targets, such as vesicles, viruses and cells, particularly where the radical diffusion length is smaller than or comparable to the collision radius. The development is exemplified with new work on inactivation of T7 bacteriophage by 25 Mev electrons and photodynamic inactivation of Saccharomyces cerevisiae. Detailed studies on yeast have shown that the sensitivity to singlet oxygen attack depends on the temperature and the culture growth phase. Spin label ESR measurements indicate that the conditions of low photosensitivity parallel low membrane fluidity. Photodynamic action measurements are being carried out with 8-methoxypsoralen (8-MOP) emphasizing the primary steps. The 8-MOP triplet state has been populated by energy transfer from acetophenone and shown to react with thymine. New work on lysozyme inactivation photosensitized by 8-MOP confirms the importance of singlet oxygen as the major damaging intermediate. In related work, 8-MOP and other psoralen derivatives were shown to be anoxic radiosensitizers of T7 phage under protective medium conditions. The results indicate that psoralens promote DNA cross link formations under the action of ionizing radiation.

TABLE OF CONTENTS

INTRODUCTION

This report summarizes research progress in the Biophysics Laboratory of the IIT Department of Physics for the approximate 15 month period starting July 1, 1976. The scientific staff of the Laboratory includes Dr. L.I. Grossweiner (Professor of Physics and Chairman of the Department), Dr. J.F. Baugher (Assistant Professor of Physics), Dr. G.E. Cohn (Assistant Professor of Physics) Dr. J.Y Lee (Research Associate), Dr. G. Goyal (Research Associate), the IIT graduate students D. Becker, J. Collins, (Miss) H.Y. Tseng, A.F. Tien, and E. Zickgraf, and laboratory technicians (Miss) L.S. Hsieh and P. Kopera. The Biophysics Laboratory collaborates with Michael Reese Medical Center in connection with pulse radiolysis and related ionizing radiation studies, particularly Dr. J. Ovadia (Director, Department of Medical Physics and Adjunct Professor of Physics, IIT) and Dr. J.L. Redpath (Attending Physician, Department of Radiation Oncology). The research projects designated by * were supported primarily by ERDA Contract No. E(11-1)-2217. The other projects are based on other support where the contributions of the Principal Investigator were partially supported by ERDA.

RESEARCH PROGRESS

1. Photoionization of Proteins and Amino Acids in Aqueous Solution*

Previous work in this laboratory has demonstrated that photoionization of aromatic amino acid residues is the major initial photochemical process in many proteins (e.g., the review of Grossweiner, 1976). The ejected electrons have been observed as hydrated electrons (e^-_{aq}) and the disulfide bridge electron adduct ($RSSR^-$) accompanied by the spectra of the 1-electron oxidation products of tryptophan (Trp^+) and/or tyrosine ($Tyr\cdot$). A summary of current results obtained by laser flash photolysis at 265 nm is given in Table I. (The laser apparatus is described in the previous Progress Report for the period 8/1/75-6/30/76.) The photochemical generation of hydrated electrons from proteins leads to important conclusions relevant to photobiology at the molecular and cellular levels:

(1) Irradiation of cells at longer wavelengths than are absorbed by DNA ($\lambda > 300$ nm) can generate superoxide (O_2^-) and hydrogen peroxide as toxic photoproducts.

(2) The photooxidation of tryptophan (TRP) to N-formylkynurenine (FK) can lead to internal photosensitization at $\lambda > 320$ nm and the generation of O_2^- and excited singlet oxygen ($^1O_2$) as damaging intermediates.

The reaction sequence of (1) is:

$$e^-_{aq} \xrightarrow[O_2]{} O_2^- \longrightarrow H_2O_2 \qquad \text{(I)}$$

which should be important for any photolysis process in which e^-_{aq} is generated under aerobic conditions. The reactions pertinent to (2) proposed by workers in this laboratory (Walrant et al., 1975) are:

Protein	Initial Quantum Yields (265 nm)					$t_{1/2}(e^-_{aq})$
	Trp^+ (a)	Trp· (b)	Tyr· (a)	e^-_{aq} (c)	$-SS^-$ (a)	nsec
lysozyme	0.023	0.031	-	0.019	0.007	210
trypsin	0.049	0.044	-	0.042	0.007	400
papain	0.044	0.025	-	0.038	0.003	560
carbonic anhydrase	0.00	0.052	-	0.024	0.005	290
subtilisin Carlsberg	0.032	0.027	0.064	0.048	-	400
subtilisin Novo	0.037	0.066	0.025	0.052	-	370
subtilisin BPN'	0.017	0.032	0.032	0.046	-	360
RNase A						
pH 6	-	-	0.015	0.015	-	600
pH 11	-	-	0.031	0.031	-	400
Catalase	-	-	-	0.059	-	700
Histone	-	-	0.035	0.026	-	100

(a) O_2, 50 nsec

(b) O_2, 2 μsec

(c) N_2, 50 nsec

Table I. Initial Quantum Yields from Laser Flash Photolysis of Proteins

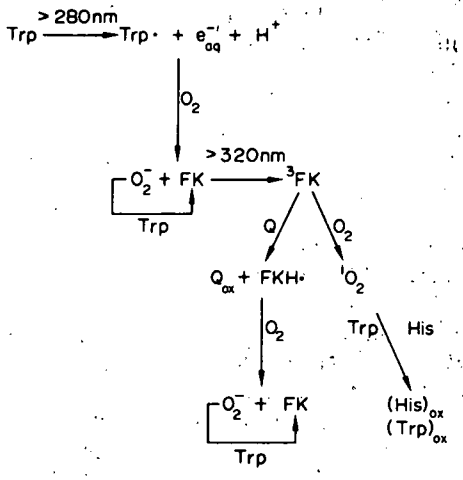

(II)

Proposed scheme for internal photosensitization in bovine carbonic anhydrase and other tryptophan-containing proteins.

Numerous studies have shown that the photochemical products generated by irradiating TRP from the near-ultraviolet to the visible regions can induce biological effects on isolated cells, including mutagenicity, inhibition of DNA strand-break repair in E. coli, and inhibition of growth and lethality to cultured mammalian cells. This literature is reviewed by McCormick et al. (1976), who propose that H_2O_2 is the toxic product. Other workers do not agree that H_2O_2 is the cytoxic agent (Zigman, et al. (1977). However, there is independent evidence that $^1O_2$, a sensitized product of TRP photooxidation via FK, inactivates yeast (Ito and Kobayashi, 1974; Cohn, et al. 1977) and is involved in the hemolysis of human erythrocytes (Michelson and Durosay, 1977).

In addition to the generation of toxic products, the photolysis of aromatic residues may have a significant effect on the functional protein absorbing the radiation. A long-term study in this laboratory on the ultraviolet inactivation of enzymes based on xenon lamp flash techniques was updated and summarized in the previous Progress Report and by Grossweiner, et al. (1976). The following general conclusions were made in that work:

(1) The numbers of photoionized TRP or TYR residues in a given protein are comparable to the exposure as measured with conventional techniques.

(2) The photolysis of TRP or TYR leads to inactivation of the enzyme when the residue is essential (e.g. lysozyme and papain) or located immediately adjacent to a key catalytic residue (e.g. trypsin). On the other hand, the photo-oxidation of TYR in RNase is not an important inactivating step, consistent with the long distance of the 3 exposed TYR residues from the active site. However, the single TRP residue in subtilisin Carlsberg is photosensitive, despite the distance from the active site region. In this case it was suggested that the photoelectron attacks the essential histidine residue.

The above considerations based on detailed analysis of flash photolytic and steady irradiation product yields in terms of the enzyme microstructures, indicate that the flash photolysis method can provide new information about photoinactivation mechanisms and the functional properties of the native enzyme. These studies have been extended with laser flash photolysis to improve the time resolution from 5 μsec as available with the xenon flash lamp-photographic plate detection method to 20 nsec with the more sensitive photoelectric detection method.

The interpretation of the protein results in Table I requires understanding the initial photochemistry of the aromatic amino acids TRP, TYR, and the influence of available disulfide reactivity. A great deal of previous work on aqueous TRP derivatives summarized by Grossweiner (1976) has led to the identification of the radical cation Trp^+ (580 nm), the neutral radical Trp· (510 nm), and the triplet state ^3Trp (460 nm), including the radical extinction coefficients and pK_a. However, there is no general agreement as to the origin of the electron or the nature of the primary photoionization act. The recent work in this laboratory (Baugher and Grossweiner, 1977) indicates that monophotonic ionization from a short-lived state other than the triplet state is the principal step:

$$TRP \xrightarrow{h\nu} \{Trp\}^* \longrightarrow Trp^+ + e^-_{aq} \qquad \text{(III)}$$

where {TRP}* may be the fluorescent state or an exciplex formed prior to (or in competition with) the fluorescent state. The consideration of the rate constants: $k(e^-_{aq} + Trp^+) \gtrsim 3 \times 10^{10}$ $\underline{M}^{-1}sec^{-1}$ and $k(e^-_{aq} + TRP) = 3.6 \times 10^8$ $\underline{M}^{-1}sec^{-1}$ shows that a substantial degree of back reaction takes place under flash photolysis conditions. (The detailed analysis of e^-_{aq} decay data for laser photolysis of various solutes led to inconsistencies with homogeneous reaction kinetics and the conclusion that the back reaction is significant even for low-intensity steady state irradiations; see section 2 below.) However, if the electron reacts with the radical, then e^-_{aq} scavengers such as H^+, 0_2 and N_20 should <u>enhance</u> the radical yields measured after the electron has decayed. (For example, in the photolysis of aqueous I^-, the yield of permanent products is promoted by e^-_{aq} scavengers.) However, flash photolysis spectra from several laboratories show that the Trp· yield is actually <u>lower</u> in 0_2 or N_20 than under N_2. To explain this anomaly, we have proposed that the back reaction does not immediately lead to the original TRP. Instead, a new intermediate Trp' is postulated that can oxidize the solute in turn:

$$\begin{aligned} Trp^+ + e^-_{aq} &\longrightarrow Trp' \\ Trp' + TRP &\longrightarrow Trp\cdot + Trp^- \end{aligned} \qquad \text{(IV)}$$

Although Trp' has not been identified, it is reasonable to assume it may be the triplet state or a biradical. The former would be consistent with low-temperature studies where UV irradiation of TRP leads to the aromatic radicals and ^{3}Trp phosphorescence. Alternatively, the deamination reaction of e^-_{aq} with Trp^+ may take place at the NH_3^+ site leading to a 3-indolepropionic acid radical that would not be easily distinguished from Trp·. The quantum yields in Fig. 1 are consistent with this mechanism. From <u>pH</u> 4 to <u>pH</u> 8 the initial electron yield is 0.10 ± 0.01, 20% lower than that for Trp^+. The discrepancy indicates a secondary pathway of radical formation not involving the electron. However,

Figure 1

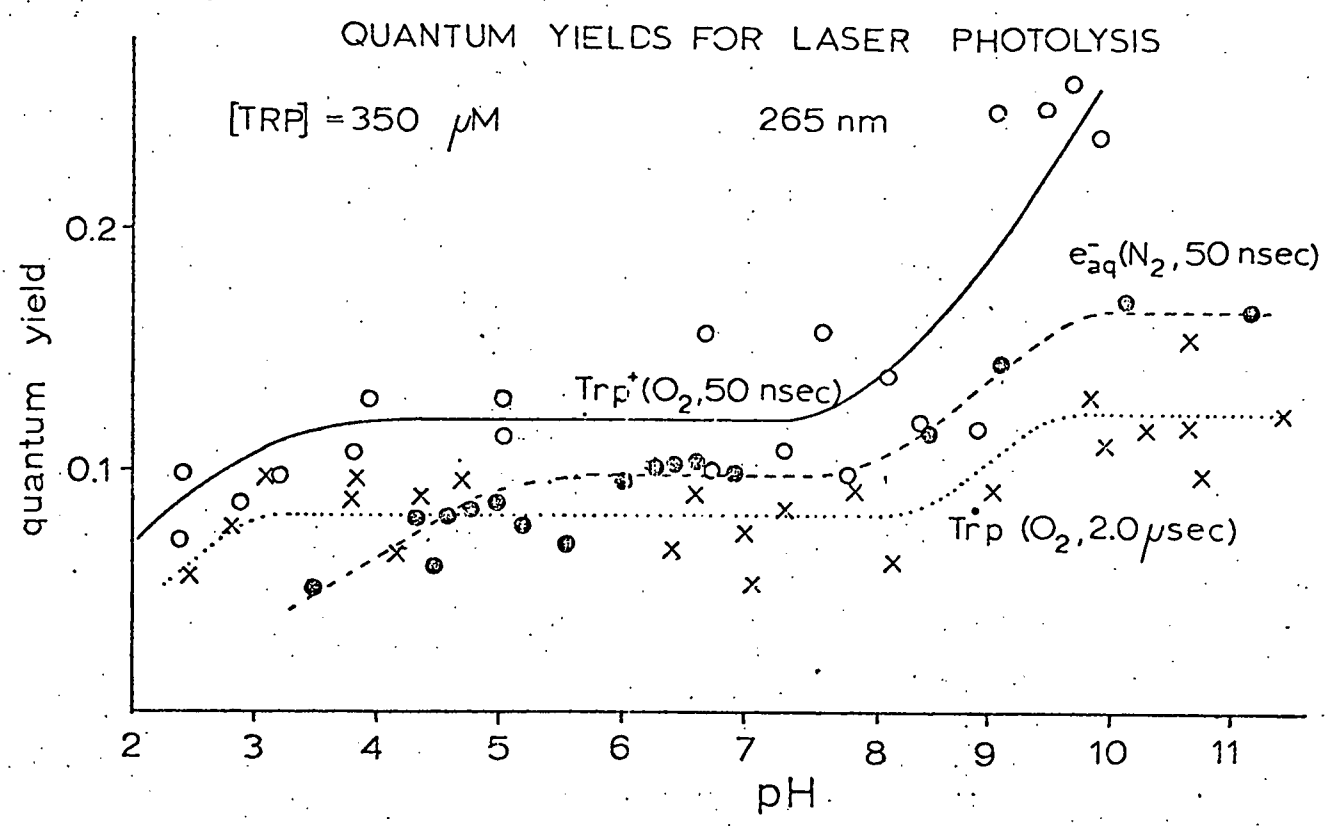

Figure 2

Dependence of electron yields on laser intensity

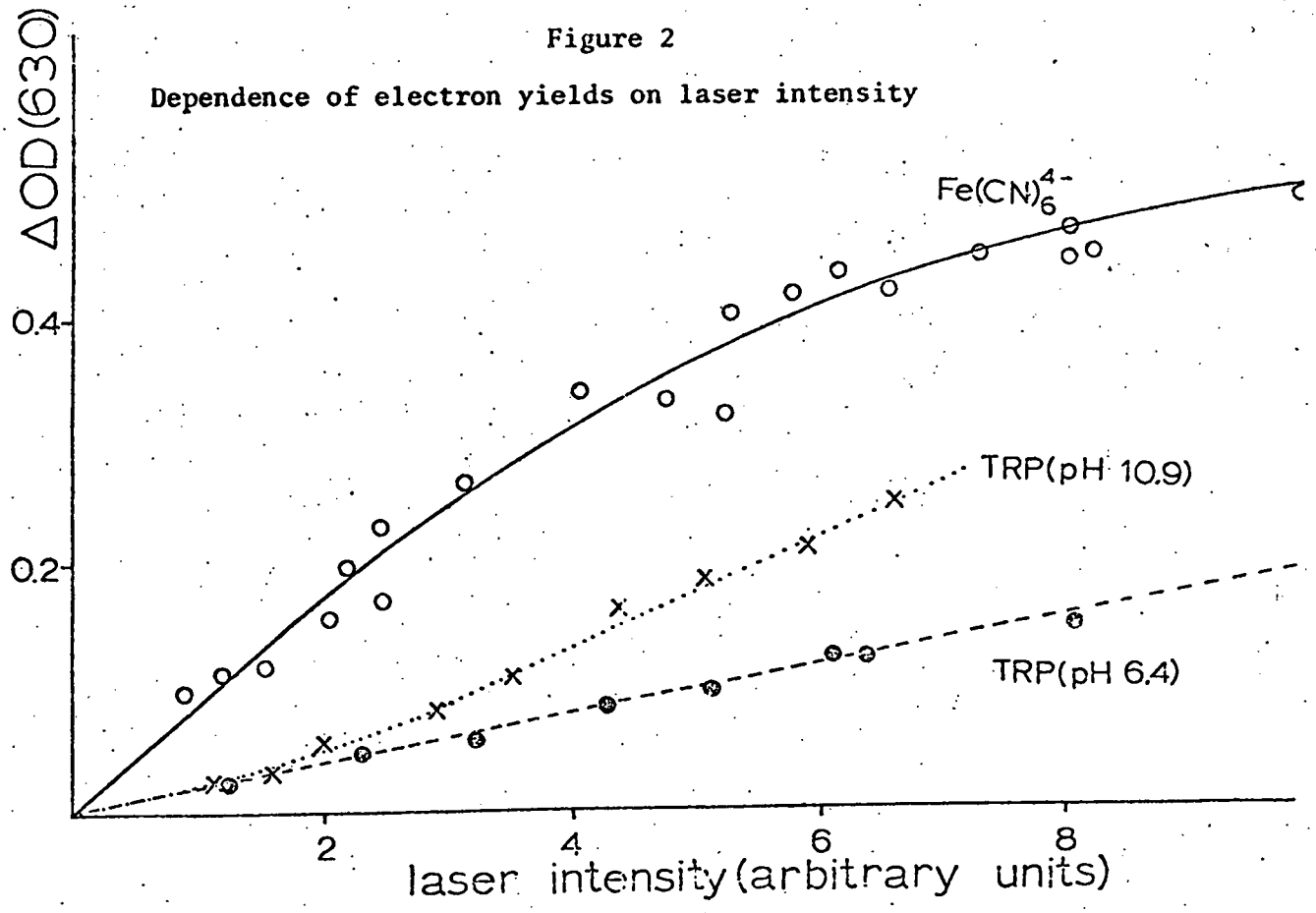

the Trp· yield is only 0.07-0.08 after 2 μsec, where the loss is attributed to electron depletion via (e^-_{aq} + TRP) and (e^-_{aq} + e^-_{aq}) which must compete with (IV). The dependence of e^-_{aq} on laser intensity in Fig. 2 shows that TRP photolysis is linear from pH 4 to pH 8. Similarly, the e^-_{aq} yield from $Fe(CN)_6^{4-}$ is linear, with saturation at high laser intensities. However, for alkaline TRP the upward curvature is indicative of a biphotonic contribution to the photoionization process, corresponding to the increase of the primary yields (Fig. 1).

The laser measurements have been extended to tyrosine and tyrosyl peptides in new work, to clarify the role of peptide bonding in the primary photolysis act. The transient spectra from tryptophyl-L-tyrosine in Fig. 3 show the phenoxyl absorption of oxidized tyrosine (Tyr·) at 410 nm and the tryptophan radicals: Trp^+ at 200 nsec and Trp· at 1.6 μsec. This result indicates that both the TYR or the TRP moieties can be photoionized, in contrast to the fluorescence of this dipeptide which is characteristic only of TRP. Assuming that the internal energy transfer takes place from the TYR relaxed, excited singlet state, the electron cannot be ejected from this state of the TYR moiety. The linear dependence of the e^-_{aq} yield from TYR on laser intensity (Fig. 4) supports this conclusion. Measurements of the e^-_{aq} and Tyr· yields (Figs. 5 and 6) show that they are equivalent in both neutral and alkaline solutions for TYR-GLY, GLY-TYR, GLY-TYR-GLY, TYR-TYR and the enzyme RNase A. However, for TYR itself, the Tyr· yield is about 50% higher than e^-_{aq} for the protonated phenolic group, indicative of an alternative photolysis pathway, presumably splitting of the O-H bond. The transient spectra L-cystinyl-bis-tyrosine (Fig. 7) has been resolved into the Tyr· and $RSSR^-$ components. However, in N_2O or O_2 the $RSSR^-$ absorption is not suppressed, indicating that the transfer of the electron from TYR to -SS- takes place via an intramolecular process not involving free e^-_{aq}. Similar non-quenching of the $RSSR^-$ absorption has been observed in lysozyme, papain, and trypsin (Grossweiner, 1976). The quantum yields in Fig. 8 indicate that the internal electron transfer is independent

Figure 3

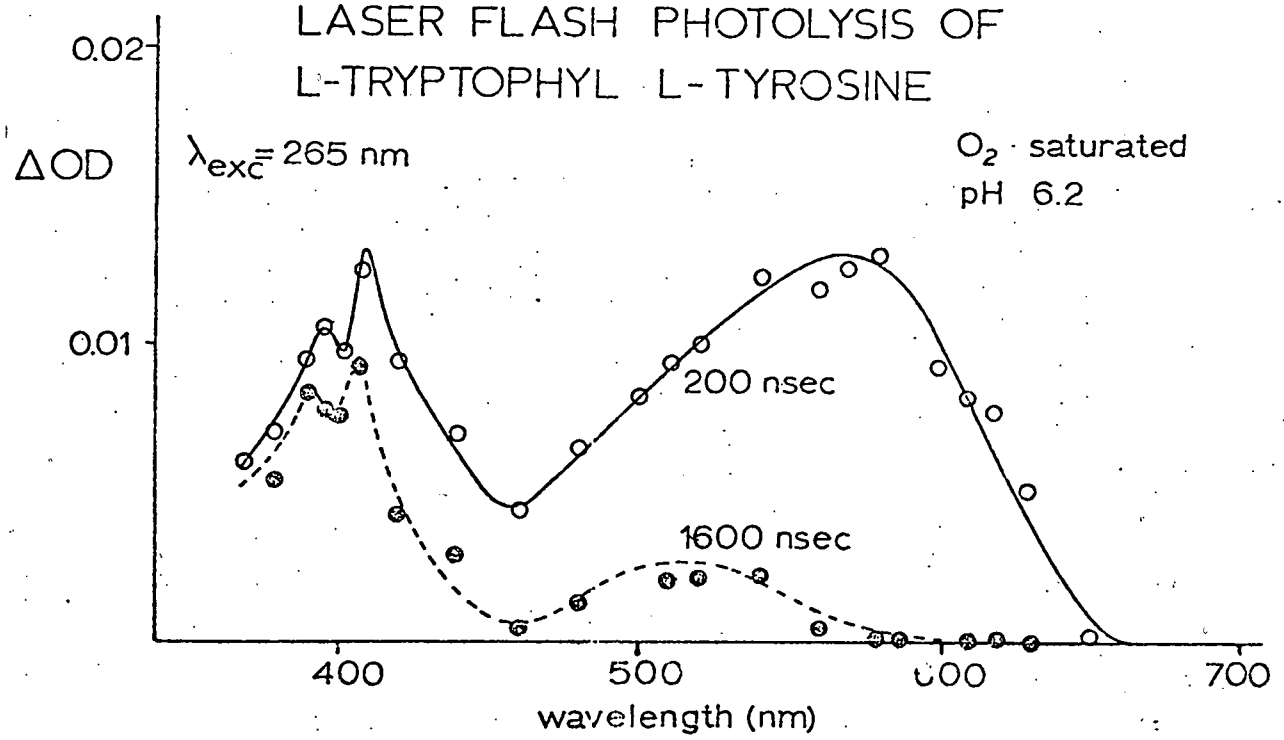

Figure 4

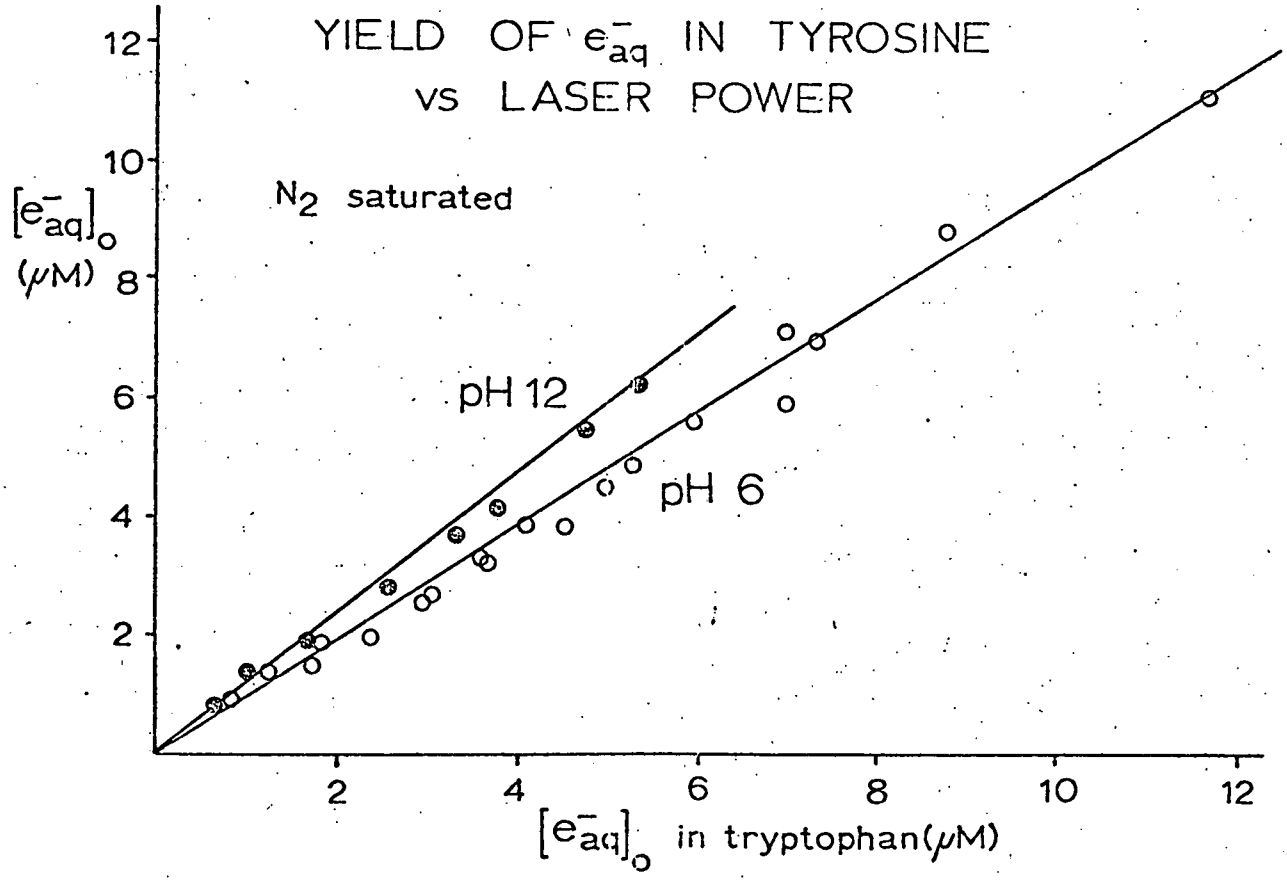

Figure 5

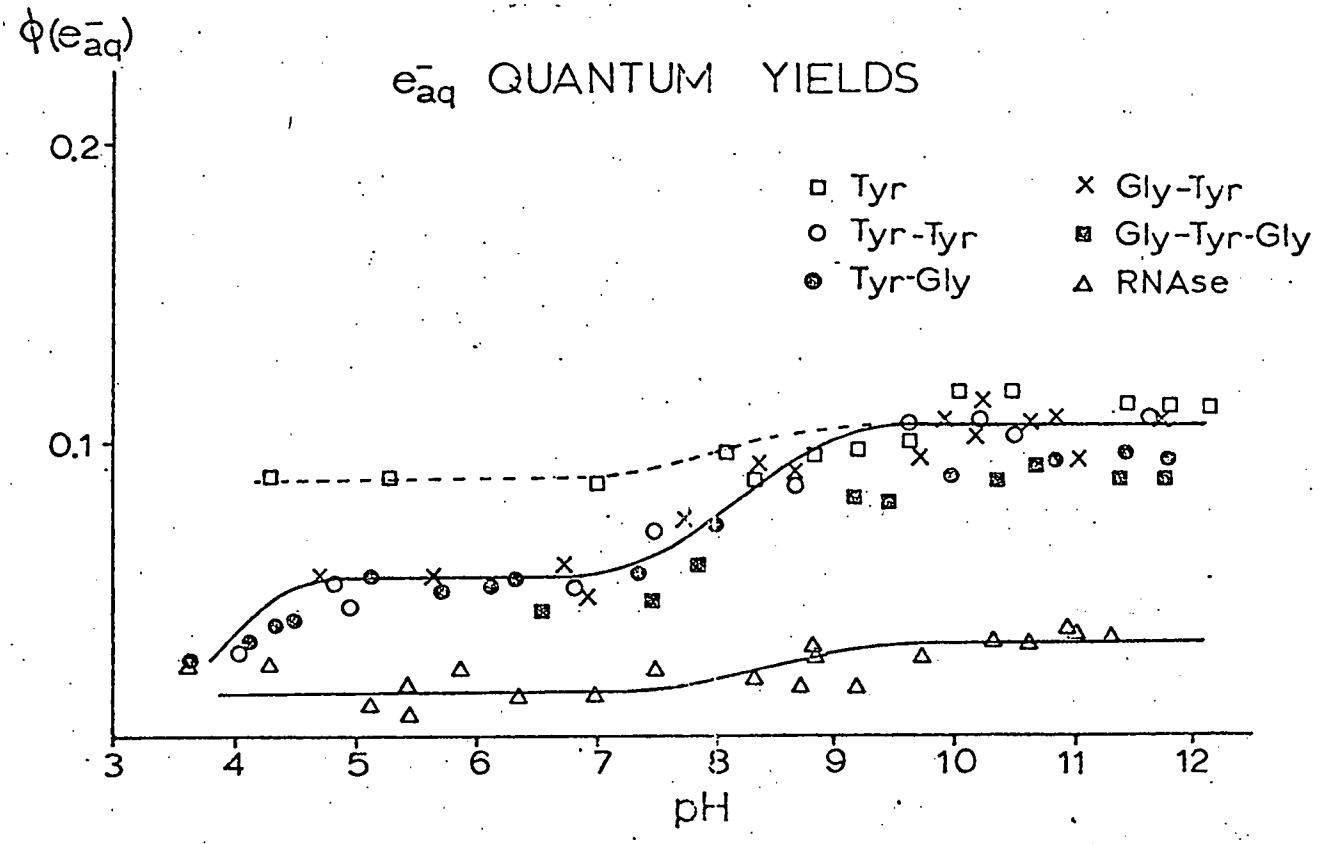

Figure 6

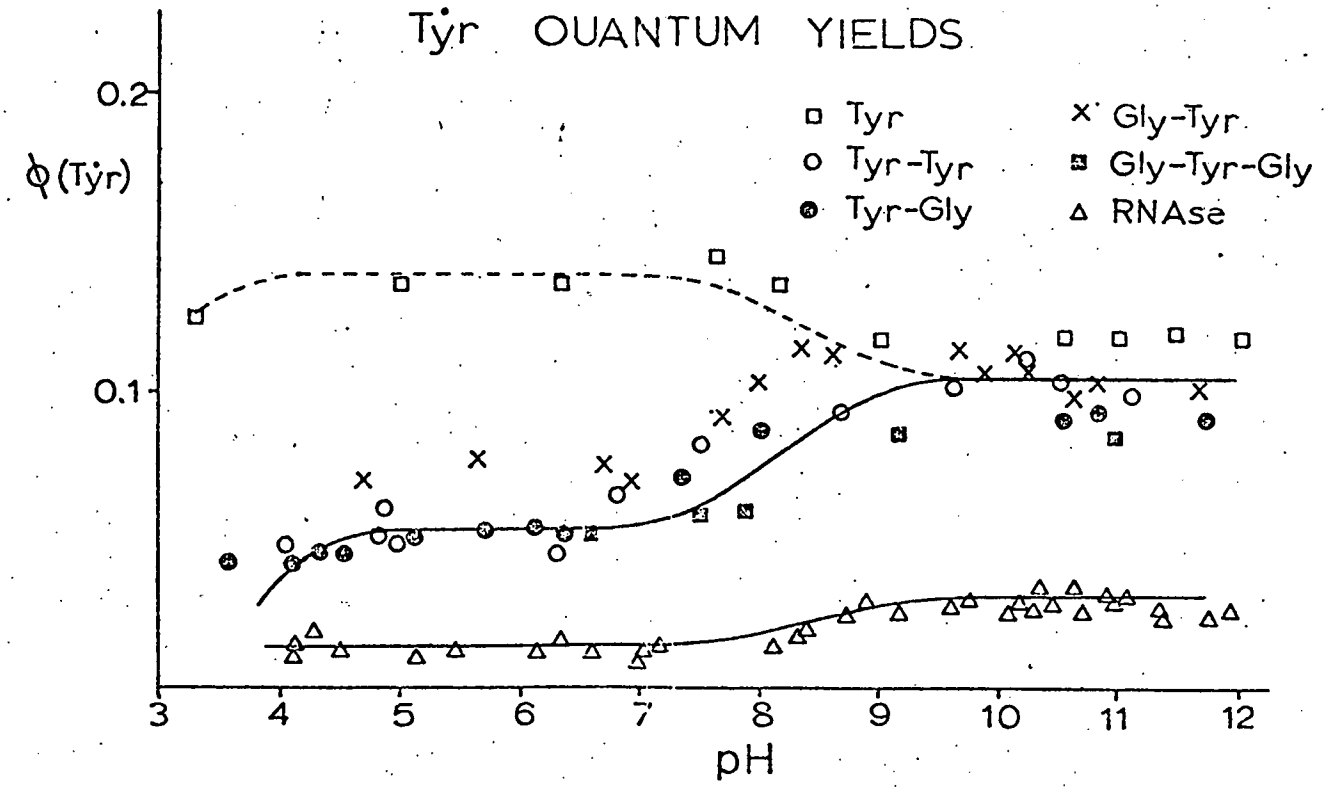

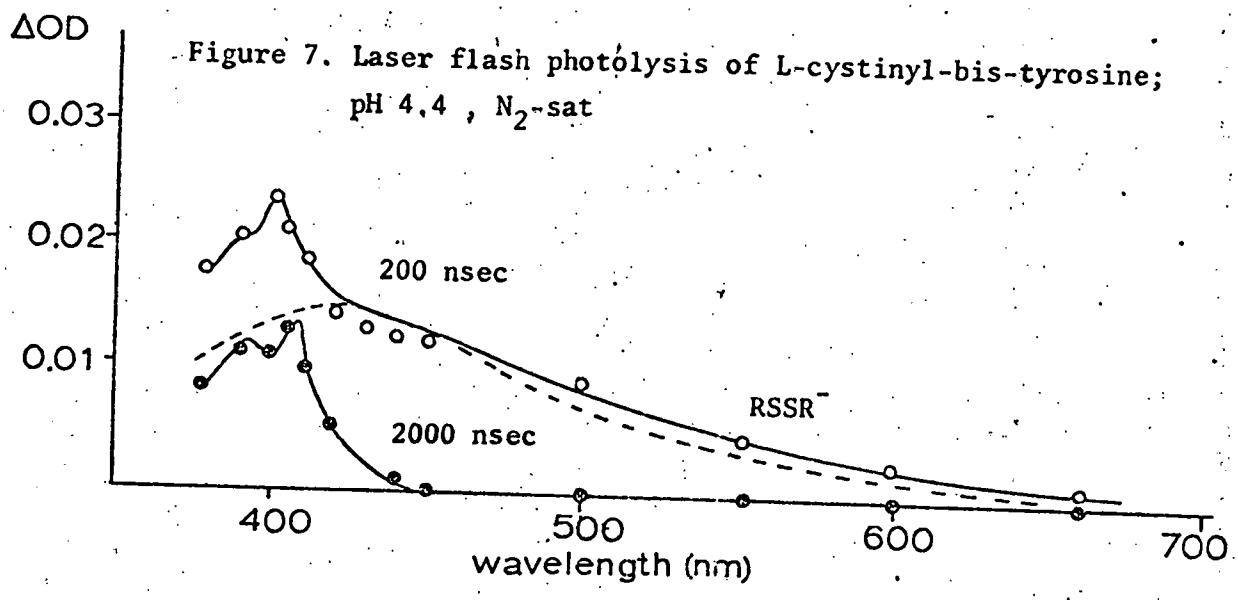

Figure 7. Laser flash photolysis of L-cystinyl-bis-tyrosine; pH 4.4 , N_2-sat

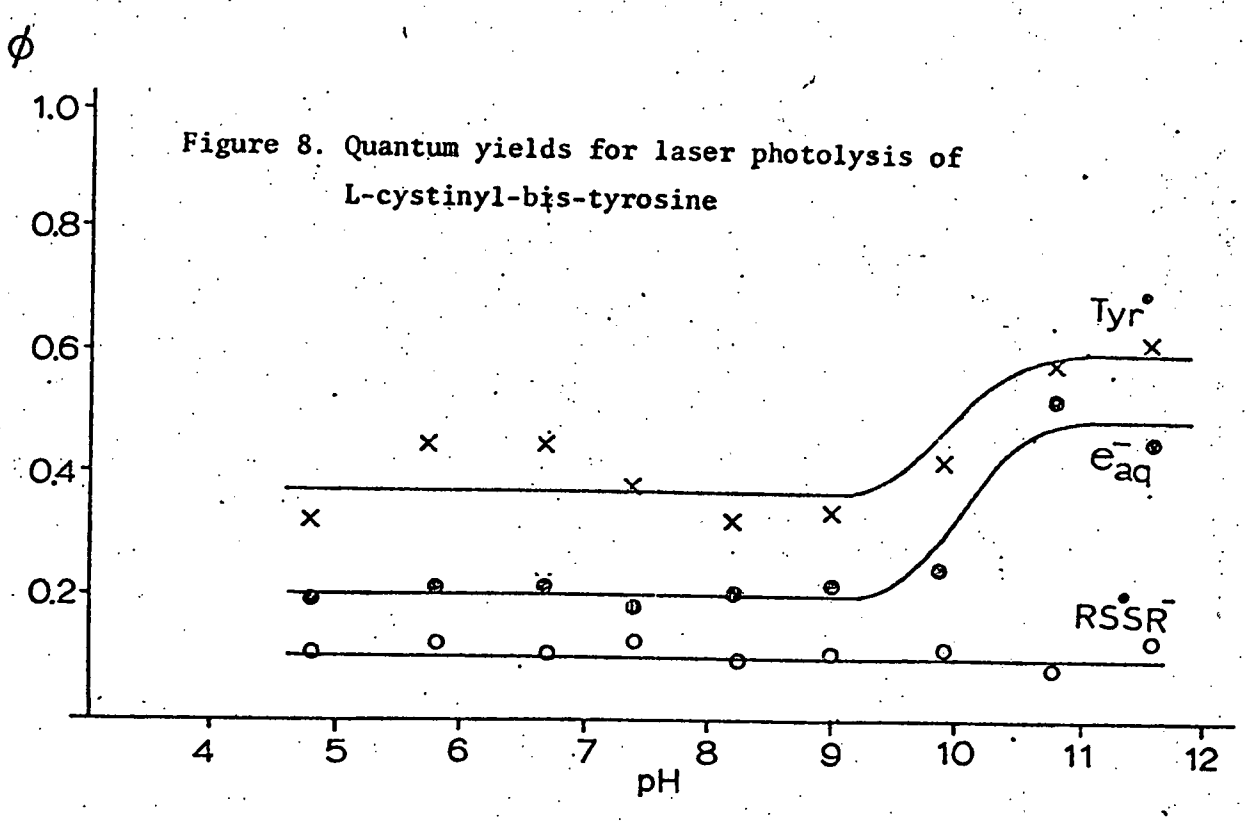

Figure 8. Quantum yields for laser photolysis of L-cystinyl-bis-tyrosine

of pH , while the e^-_{aq} and Tyr· yields increase for the anion comparable to the other tyrosine peptides.

Laser flash studies on several enzymes have led to detailed information about the photoionization process. The initial yields determined for native lysozyme and lysozyme treated with N-bromosuccinimide (NBS) are given in Table II. Previous work (Imoto, et al. 1971) indicates that of the 6 TRP residues in lysozyme, TRP-62 and TRP-108 account for about 90% of the fluorescence. The oxidation of TRP-62 by NBS induces about 50% fluorescence quenching (last column) as expected. This treatment diminishes the Trp· yield by a factor of 2 but does not significantly alter the e^-_{aq} yield. It is concluded that the electron released by TRP-108 is trapped in the medium as e^-_{aq} while the electron released from TRP-62 goes to a disulfide bridge and other internal traps. (Note that the relative e^-_{aq} yields from native lysozyme and aqueous TRP are consistent with e^-_{aq} formation from 1 of the 6 TRP residues.) These studies strongly suggest that the exposure of TRP-108 in solution is considerably higher than deduced from the crystallographic data showing that the side chain is almost completely buried.

Table II. Initial product yields for 265 nm laser photolysis of lysozyme and NBS-lysozyme

Photolyte	$\phi(e^-_{aq})$*	$\phi(Trp^{\cdot})$†	$\phi(-S^{\cdot}\ ^{\cdot}S-)$†	F‡
Lysozyme (pH 5)	0.019 ± 0.002	0.031 ± 0.003	0.007	1.0
NBS-Lysozyme (pH 5)	0.016 ± 0.002	0.015 ± 0.002	0.004	0.51 ± 0.03
Tryptophan (pH 7.4)	0.10 ± 0.01§			

* N_2-sat; 50 ns delay.
† Air-sat; 1 μs delay.
‡ Relative fluorescence efficiency; excited 285 nm, measured 340 nm.
§ From Baugher and Grossweiner (1976).

Carboxypeptidase A (CPA) has 7 TRP residues and 19 TYR residues, with a single -SS- bridge located about 20 Å from the liganded zinc atom. The initial products yields are given in Table III for the native enzyme and the apoenzyme. For CPA, the Trp· yield at 50 nsec equals the sum of e^-_{aq} plus $RSSR^-$. The number of photolabile TRP residues is: (0.057/0.63) x (7/0.10) = 6.3, where 63% of the

incident 265 nm light is absorbed by the 7 TRP residues. The corresponding number of photolabile TRP residues in the apoenzyme is: (0.044/0.63) x (7/0.10) = 4.9. It is deduced that extraction of the zinc diminishes the effective number of photoionized TRP residues by about 1 residue but does not alter either e^-_{aq} or $RSSR^-$. This result is quite surprising because none of the TRP residues appears to be involved in the catalytic mechanism or substrate binding. However, pulse radiolysis data indicate that Br_2^- oxidizes a TRP residue to Trp· in conjunction with inactivation of the enzyme (Roberts, 1973), suggesting that an exposed TRP residue interacts with the active site region through long-range conformation changes.

TABLE III. Initial Product Yields for 265 nm Laser Photolysis of CPA and apo-CPA

Photolyte	(e^-_{aq})*	(Trp·)#	$(RSSR^-)$#
CPA (pH 7.5)	0.042 ± 0.010	0.057 ± 0.001	0.013 ± 0.006
apo-CPA (pH 7.5)	0.039 ± 0.002	0.044 ± 0.004	0.010 ± 0.004
Tryptophan (pH 7.4)	0.10 ± 0.01**	-	-

* N_2-sat; 50 ns delay

\# Air-sat; 1 μs delay

** From Baugher and Grossweiner (1977)

2. Non-Homogeneous Decay Reactions of the Photochemical Hydrated Electron*

The previous laser flash photolysis studies on aromatic amino acids and several inorganic anions led to the surpirsing result that the decay of the hydrated electron is significantly faster than predicted from homogeneous reactions kinetics and does not follow the expected dependence on initial e^-_{aq} concentration and scavenger concentrations. (Bryant et al., 1975). The decay curves were approximately exponential in the initial stage for TRP, TYR, 1-MethylTRP, I^-, and $Fe(CN)_6^{4-}$ with about the same lifetime for all solutes ($\sim$1 μsec), which increases with temperature at the same activation energy as the "inverse viscosity" of water. Furthermore, measurements of radical and e^-_{aq} decays for TRP and 1-MethylTRP indicate that they react together during the initial decay period. In retrospect, this is not an unexpected result because homogeneous kinetics predicts that $k(e^-_{aq} + Trp^+) \simeq 3 \times 10^{10}$ $\underline{M}^{-1}sec^{-1}$ competes with $k(e^-_{aq} + TRP) = 3.6 \times 10^8$ $\underline{M}^{-1}sec^{-1}$ under flash photolysis conditions with $(e^-_{aq})_o = 5 - 50$ μ$\underline{M}$. However, the approximately constant decay lifetime for all of these solutes is not explained, particularly because e^-_{aq} does not react with the photolyte for the cases of I^- and $Fe(CN)_6^{4-}$.

Prior to flash photolysis studies, Stein and his colleagues (Jortner, et al. 1962 a,b,c,d, 1963, 1964) proposed that hydrated electrons are generated from aqueous halide ions and phenolate ion, based on steady irradiation product yields in the presence of added electron scavengers such as O_2 or N_2O. The quantum yield of electron scavenging was found to obey the square-root concentration dependence predicted by the Noyes (1955, 1956, 1961) theory of diffusive recombination, in which the geminate co-products escaping primary recombination undergo secondary diffusive recombination in competition with scavenging in the "cage" and diffusive separation into the bulk. According to Noyes, the efficiency of scavenger action is given by: $\int_0^\infty h(t') \left[1 - e^{-k_s(S)t'} \right] dt'$, where h(t) is the probability

(per sec) that a radical pair generated at t = 0 (or interacting at t = 0 without reaction) recombines at time t, k_s is the bimolecular rate constant for the scavenging reaction, and (S) is the scavenger concentration. The choice of h(t) based on the random walk of a particle in 3 dimensions:

$$h(t) = (a/t^{3/2})e^{-a^2/\beta'^2 t} \tag{1}$$

leads to the approximate solution:

$$\gamma = \gamma_r + 2a\Gamma\sqrt{\pi k_s(S)} + \ldots \tag{2}$$

where γ is the total quantum yield for electron scavenging, γ_r is the "residual yield" for the scavenging of electrons that escape recombination at low scavenger concentrations, and Γ is the quantum yield for generation of the geminate radicals. The parameter β' is the total probability for recombination of the geminate pair:

$$\beta' = \int_0^\infty h(t')dt' \tag{3}$$

and is related to the photochemical quantum yields by: $\beta' = 1 - \gamma_r/\Gamma$. Jortner, et al. (1962a)obtained the exact solution of (1):

$$\gamma = \Gamma\left[1 - \beta' e^{-(2a/\beta')\sqrt{\pi k_s(S)}}\right] \tag{4}$$

which reduces to (2) at low scavenger concentrations.

The functional dependence predicted by (2) or (4) was found for various photolytes (I^-, Br^-, $Fe(CN)_6^{4-}$, phenolate) in the presence of electron scavengers (H^+, N_2O, O_2, $H_2PO_4^-$, acetone) with approximately correct relative values of k_s from system to system. However, the key parameter $2a\sqrt{\pi k_s}$ ranges from 2 to 60 $(\text{liters/mole})^{\frac{1}{2}}$, which is much too large to be consistent with the Noyes theory of diffusive displacements. The experimental results imply values of $a \sim 10^{-4}$ $\text{sec}^{\frac{1}{2}}$ and "cage" lifetimes $\sim 10^{-6}$ sec, while the Noyes theory leads to a $<10^{-6}$ and lifetimes $<10^{-10}$ sec. Nevertheless, there has been no apparent explanation for the

discrepancy excluding the total inapplicability of the diffusive recombination theory. Dainton and Logan (1965) proposed an alternative mechanism in which the rapid reaction of the photoelectron with a scavenger may not permit adequate time for the formation of the ionic atmosphere of the electron, leading to a decreased rate constant for scavenging by charged solutes at high solute concentrations. However, this model does not explain the square-root concentration dependence of scavenging quantum yields observed by Stein and co-workers.

In photochemical scavenging experiments the reactions of the photoelectron are inferred by measuring the ability of added scavengers to compete with electron back reactions. Laser flash photolysis provides a direct probe of the same process, where the decay of the electron and the effect of scavengers on the decay process are monitored by absorption spectroscopy. The apparently inconsistent long lifetimes of the electron estimated by applying Noyes theory to photochemical scavenging yields are, in fact, quite consistent with the laser flash photolysis results. Accordingly, Grossweiner and Baugher (1977) proposed the inapplicability of the "solvent cage" model does not rule out applying the Noyes mathematical approach in the longer time regime, where the long-range diffusion of the electron through the medium competes with inhomogeneous electron-radical back reactions and pseudo-first order scavenging reactions.

We first consider the case where the geminate pairs are sufficiently separated so that only reactions of the electron with the original radical compete with scavenging in the bulk by the photolyte and/or added solutes. The probability that an electron survives both decay process from t = 0 to t = t is given by:

$$p(t) = e^{-k_s(S)t} \left[1 - \int_0^t h(t')dt' \right] \tag{5}$$

We proceed formally by substituting h(t) of (1) leading to the decay function:

$$p(t) = e^{-k_s(S)t} \left[1 - \beta' \operatorname{erfc} (a/\beta') \sqrt{\pi/t} \right] \tag{6}$$

where erfc $x = (2/\sqrt{\pi}) \int_x^\infty e^{-x^2}\, dx$. The expansion: erfc $x = 1 - (2x/\sqrt{\pi})$ $[1 - x^2/3 + x^4/10 - \ldots]$ leads to an approximate form of (6) valid for $t \gg \pi a^2/\beta'^2$:

$$p(t) \simeq e^{-k_s(S)t} \left[1 - \beta' + 2a/\sqrt{t}\right] \tag{7}$$

These equations predict that the electron decay function is the product of the exponential rate as determined by reactions with scavenger S (which may be the photolyte) modulated by a scavenger-independent term related to the diffusive back reaction of the original pair. Although the decay predicted by (6) is non-exponential, the mean electron lifetime can be defined as:

$$\bar{t} = \int_0^\infty t\,dp \;\Big/\; \int_0^\infty dp \tag{8}$$

The integrations in (8) are easily carried out using (1), (5) and the approximation of (7) for the $\left[1 - \int_0^t h(t')dt'\right]$ term in dp leading to

$$\bar{t} = \frac{a\sqrt{\pi/k_s(S)}\left[1 + e^{-(2a/\beta')\sqrt{\pi k_s(S)}}\right] + (1 - \beta')/k_s(S)}{2a\sqrt{\pi k_s(S)} + \beta' e^{-(2a/\beta')\sqrt{\pi k_s(S)}} + (1 - \beta')}$$

[Formally, each of the 6 integrals in (8) is a Laplace transform L_p with $p = k_s(S)$.] In comparing the predicted dependence of $\bar{t}$ on (S) with experimental data it is convenient to use the reciprocal form:

$$1/\bar{t} = k_s(S)\, \frac{\beta' e^{-(2a/\beta')\sqrt{\pi k_s(S)}} + 2a\sqrt{\pi k_s(S)} + (1 - \beta')}{a\sqrt{\pi k_s(S)}\left[1 + e^{-(2a/\beta')\sqrt{\pi k_s(S)}}\right] + (1 - \beta')} \tag{9}$$

The probability that a pair eventually recombines is also of interest. Since $(\gamma-\gamma_r)/\Gamma$ is the probability for scavenging and γ_r/Γ is the probability that the electron escapes both recombination and scavenging, the recombination p_r follows from (4) as:

$$p_r = \beta' e^{-2(a/\beta')\sqrt{\pi k_s(S)}} \tag{10}$$

Alternatively, the same result can be calculated directly from $p_r = \int_0^\infty h(t)e^{-k_s(S)t}\,dt$.

The attempt to calculate $\bar{t}$ in the absence of scavengers by substituting (1) in (8) leads to a divergent integral. This result is not surprising because h(t) is based on ramdon walk in 3 dimensions, in which there is a finite probability that two particles executing independent steps will never meet. Nevertheless, the mean electron lifetime in the absence of scavengers can be estimated as the time required for the integrated probability of recombination to attain half the maximum value. Taking $\int_0^{t'} h(t)dt = \beta'/2$ gives:

$$t' \simeq 13.8\ (a/\beta')^2 \tag{11}$$

For example, if a/β' equals 10^{-6}, 10^{-5}, or 10^{-4} $sec^{\frac{1}{2}}$, the corresponding electron lifetimes are 10^{-11}, 10^{-9}, and 10^{-7} sec, respectively.

The decay function (6) has only two arbitrary parameters: β' is the probability of electron-radical back reaction in the absence of scavengers and has been taken as unity. [The decay curves are not sensitive to the specific value of β' with an appropriate change of the a-parameter (Grossweiner and Baugher, 1977)]. The a-parameter which is related to the electron lifetime was adjusted for a good fit to the data. Typical results for laser photolysis of $Fe(CN)_6^{4-}$ (Fig. 9), various TRP concentrations (Fig. 10), TYR (Fig. 11), and alkaline TRP and TYR (Fig. 11) are in good agreement with the predictions, particularly for the initial stages of the decay period. The values of the a-parameter in Table IV are relatively independent of the photolyte, as expected if the electron lifetime is controlled

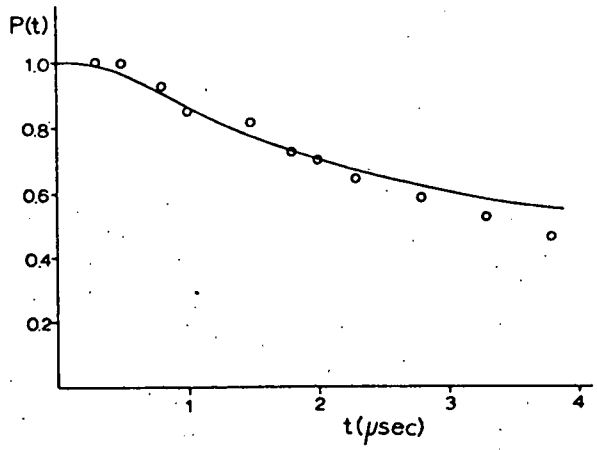

Figure 9. Comparison of eq 6 with electron decay after 265-nm laser photolysis of aqueous 0.66 M $K_4Fe(CN)_6^{4-}$. The line is calculated for $\beta' = 1$ and $\bar{a} = 5.8 \times 10^{-4}$.

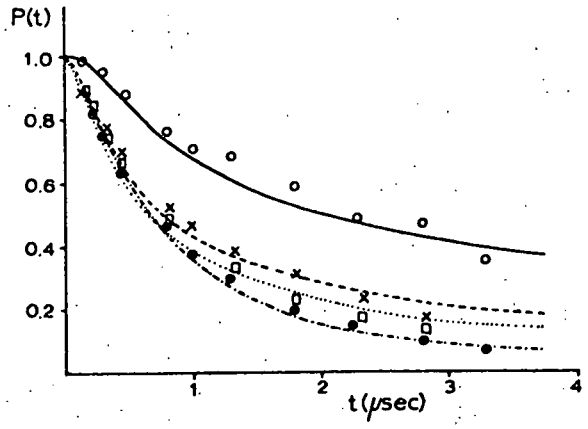

Figure 10. Comparison of eq 6 with electron decay after 265-nm laser photolysis of aqueous tryptophan at different initial concentrations: (O) 71 μM; (X) 330 μM; (□) 568 μM; (●) 1500 μM. The $\bar{a}$ values are in Table V.

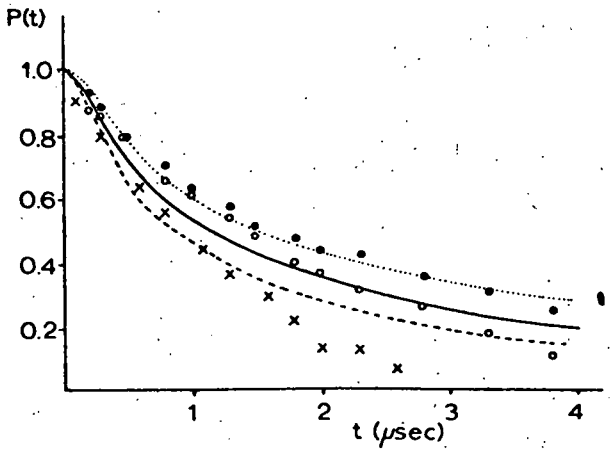

Figure 11. Comparison of eq 6 with electron decay after 265-nm laser photolysis of: 350 μM tryptophan at pH 10.9 (●, dotted line); 1560 μM aqueous tyrosine (X, dashed line); 1300 μM tyrosine at pH 11.0 (O, solid line). The lines are calculated with eq 6 using $\bar{a}$ values in Table V.

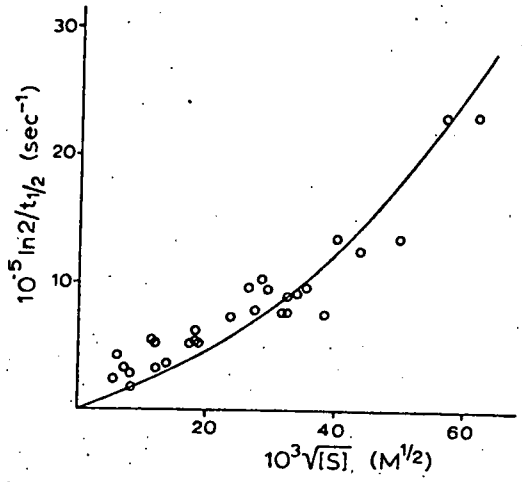

Figure 12. Dependence of experimental electron decay lifetimes on square-root tryptophan concentration. The solid line is based on eq 9 for $\beta' = 1$, $k_s = 3.6 \times 10^8$, and $\bar{a} = 3.0 \times 10^{-4}$.

TABLE IV. Summary of Electron Decay Results

Photolyte	pH	$(e_{aq}^-)_0$, μM	$10^4\bar{a}$,[a] $s^{1/2}$
71 μM tryptophan	Aq	2.8	4.1
132 μM tryptophan	Aq	4.7	2.8
330 μM tryptophan	Aq	6.4	2.5
568 μM tryptophan	Aq	7.9	2.5
1500 μM tryptophan	Aq	7.1	3.4
350 μM tryptophan	10.9	5.8	3.5
1560 μM tyrosine	Aq	3.2	4.1
1300 μM tyrosine	11.0	10.7	3.4
0.2 M I^-	Aq	11.3	4.2
660 μM $Fe(CN)_6^{4-}$	Aq	7.4	5.8

[a] Based on eq 6 with $\beta' = 1$.

by the diffusion through the medium. The measured dependence of the electron lifetime on the TRP concentration (Fig. 12) is in good agreement with the prediction of (9) taking $a = 3 \times 10^{-4}$ $sec^{\frac{1}{2}}$ from the decay data.

The departure of the decay curves from (6), particularly at high initial e^-_{aq} yields, is attributed to the onset of bimolecular reactions where the electrons have time to react with electrons or radicals generated in other pairs. This case was treated by introducing into the decay equation for homogeneous first-order and second-order electron decay reactions the time dependent rate constant equivalent to (6):

$$\frac{dp}{dt} = - \left[k_s(S) + \frac{h(t)}{1 - \int_0^t h(t')dt'} \right] p(t) \equiv - k_t p(t)$$

For the case where $t \gg \pi a^2/\beta'^2$:

$$k_t \simeq k_s(S) + \frac{1}{2t + (t^{3/2}/a)\ (1 - \beta')} \tag{12}$$

The bimolecular contribution to electron decay may be estimated for the case of high recombination probability by substituting the binomial expansion of (12) into the differential rate equation:

$$-d(e^-_{aq})/dt = k_t(e^-_{aq}) + k'(e^-_{aq})^2 \tag{13}$$

leading to the integrated solution for the case where $\gamma \equiv (1 - \beta')/2a \ll \sqrt{t}$:

$$(e^-_{aq})/(e^-_{aq})_o = \frac{\sqrt{t_o/t}\ e^{-k_s(S)t + \gamma\sqrt{t}}}{e^{-k_s(S)t_o + \gamma\sqrt{t_o}} + k'(e^-_{aq})_o e^{\gamma^2/4k_s(S)} \sqrt{\pi t_o/k_s(S)} \left[\text{erf } x - \text{erf } x_o \right]} \tag{14}$$

where $x \equiv \sqrt{k_s(S)t} - \gamma/\sqrt{4k_s(S)}$ and t_o is an arbitrary starting time corresponding to $(e^-_{aq})_o$. A reduced form of (14) for low scavenger concentrations and high recombination probability is:

$$(e^-_{aq})/(e^-_{aq})_o = \frac{\sqrt{t_o/t}}{1 + 2k' (e^-_{aq})_o t_o \left[\sqrt{t/t_o} - 1\right]} \qquad (15)$$

which predicts the dependence of the decay halftime on $(e^-_{aq})_o$ as:

$$k' (e^-_{aq})_o \, t_{\frac{1}{2}} + \left[1/\sqrt{4t_o} - k'(e^-_{aq})_o\sqrt{t_o}\right] \sqrt{t_{\frac{1}{2}}} = 1 \qquad (16)$$

Comparing (15) with (7) for low initial electron yields indicates $t_o \simeq 4a^2$, consistent with $t \int_o^\infty a/t^{3/2}\, dt = 1$.

The experimental points in Fig. 13 for the dependence of the e^-_{aq} lifetime from 350 M TRP on the initial e^-_{aq} yield are in good agreement with (16) taking $k(e^-_{aq} + e^-_{aq}) = 1.1 \times 10^{10}$ $\underline{M}^{-1}sec^{-1}$ and $a = 3 \times 10^{-4}$ $sec^{\frac{1}{2}}$. The observed variation of $t_{\frac{1}{2}}$ from 1.2 μsec at $(e^-_{aq})_o$ = 5 μM to 0.7 μsec at $(e^-_{aq})_o$ = 20 μM differs significantly from the predictions of homogeneous kinetics where the $t_{\frac{1}{2}}$ should decrease 5 μsec to 2.5 μsec for the same (e^-_{aq}) variation. Homogeneous kinetics is in even poorer agreement for the dependence of $t_{\frac{1}{2}}$ on TRP concentration, where the data of Fig. 12 indicate that $t_{\frac{1}{2}}$ decreases from 2 μsec at (TRP) = 70 μM to 0.7 μsec at (TRP) = 1.5 mM. In this case homogeneous kinetics leads to a $t_{\frac{1}{2}}$ variation from 11 μsec to 1.2 μsec.

Critique

1. The proposed decay mechanism for photoelectrons ejected by UV irradiation of aromatic solutes and inorganic anions postulates that the electron diffuses through the medium as a quasi-free entity, where the back reaction of the electron with the original radical competes with scavenging by the photolyte and/or other solutes and reacts with electrons and radicals generated in other pairs. The

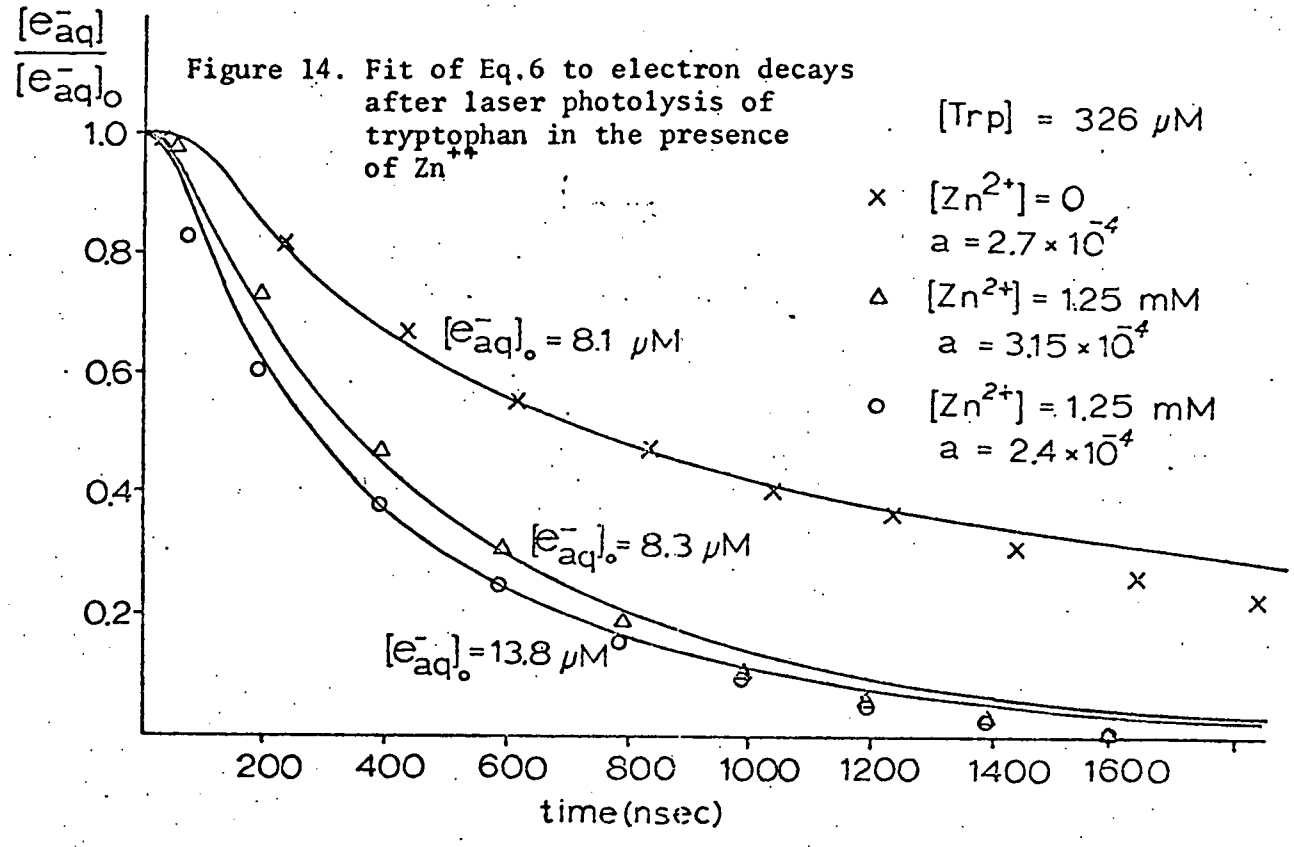

Figure 14. Fit of Eq.6 to electron decays after laser photolysis of tryptophan in the presence of Zn^{++}

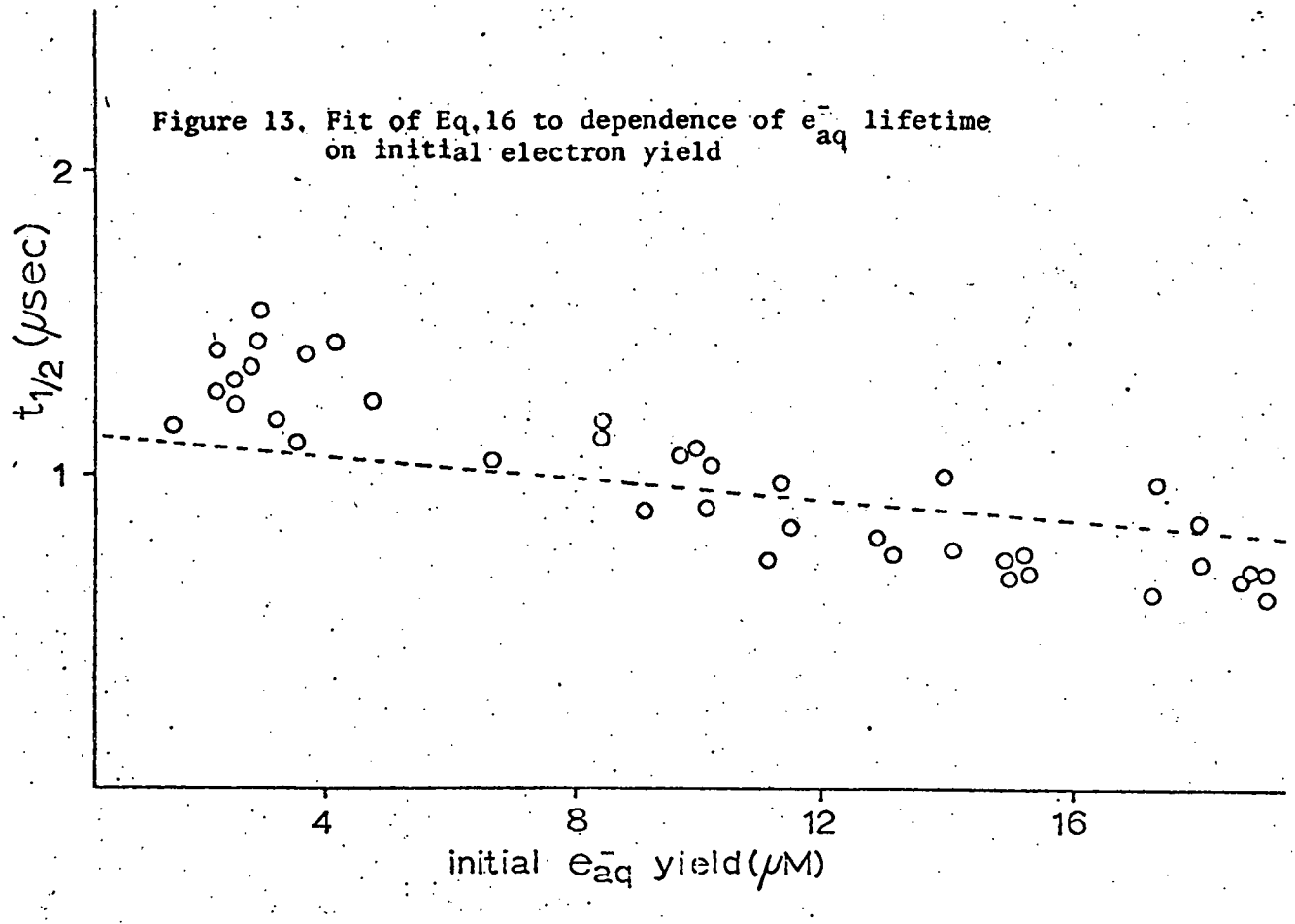

Figure 13. Fit of Eq.16 to dependence of e^-_{aq} lifetime on initial electron yield

predicted decay function and the dependence of the electron lifetime on scavenger concentrations and the initial electron concentration are in good agreement with the laser flash photolysis data obtained with I^-, $Fe(CN)_6^{4-}$, TRP and TYR in neutral and alkaline solutions.

2. The time during which original-pair back reactions take place is considerably longer than would be expected from diffusion theory. For a typical value $(e^-_{aq})_o$ = 5 μM the geminate pairs are separated by 400 Å. Taking $D(e^-_{aq})$ = 5 x 10^{-5} cm^2/sec, the electron requires about 0.05 μsec to diffuse a corresponding r.m.s. distance. The possibility cannot be excluded that this calculation is wrong and the hydrated electron has a lower mobility than indicated by the limited experimental determinations of this quantity. Assuming the high mobility is correct, it appears that the fitting procedure does not distinguish properly the limit of (6) based on only original-pair back reactions and (14) or (16) in which pair-pair interactions are included. However, it has been found that (16) fits the data as well as (6) after about 0.5 μsec delay and the numerical solution of (13) using the exact p(t) function gives a good fit over the entire time range. This result is illustrated in Fig. 14 for the decay of electrons generated from TRP in the presence of Zn^{++}.

3. The parameters a and β' determined from the e^-_{aq} decay data are consistent with the equivalent parameters based on photochemical scavenging experiments. This agreement resolves the earlier controversies over the relationship of the scavenging experiments to the Noyes' cage recombination model. If a solvent cage of $\sim 10^{-10}$ sec duration is formed during photoionization process in fluid water, no experimental evidence for its existence has been reported as yet. More likely, the large initial separation of the electron and radical after full solvation precludes the formation of this structure.

3. Kinetics of Damage to Large Biological Targets in Media*

In vitro investigations of radiation damage to large biological targets, e.g. vesicles, viruses, bacteria, yeast, and mammalian cells, are usually carried out by irradiating the sytem in dilute suspension. In ionizing radiation studies the damaging intermediates generated in the external medium must reach the target by diffusional processes, in addition to the damage induced by energy absorbed within the biological system. Similarly in photodynamic action, light absorbed by internal and external sensitizing molecules may be effective, where the diffusive processes of the external intermediates parallels the "indirect action" of ionizing radiation. The analysis of dose-response data for these cases is usually treated with competition kinetics, in which the primary species generated in the medium reacts with the biological target, in competition with scavenging by available solutes and the generation of damaging secondary species by such scavenging processes. The general case is indicated by the reaction scheme:

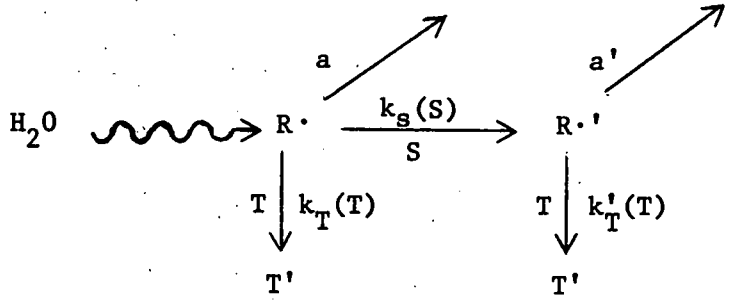

(V)

where R· is the primary radical, R·' is the secondary radical generated by reactions of R· with the scavenger S, T is the active target, T' is the damaged target, and the k's and a's are the bimolecular and psuedo-first order rate constants, respectively, for the processes shown. The straightforward application of steady-state reaction kinetics leads to:

$$G_i = -9.637 \times 10^8 \, d(T)/dD = G_R(T) \left[\eta k_T + \frac{\eta' k_T' k_s'(S')}{a' + k_T'(T)} \right] \Big/ \left[a + k_T(T) + \Sigma k_s(S) \right] \quad (17)$$

where G_i is the number of biological events per 100 ev absorbed in the medium, G_R is the number of primary radicals generated per 100 ev, D is the absorbed dose in rads, S' is the scavenger that leads to damaging secondary radicals, and the η's are the probabilities that reactions of the primary or secondary radicals with the target lead to an observable effect. The integrated solution is:

$$(T)/(T)_o = e^{-D/D_{37}} \quad (18)$$

with

$$1/D_{37} = 1.0377 \times 10^{-9} \, G_R \left[\eta k_T + \frac{\eta' k_T' k_s'(S')}{a' + k_T'(t)} \right] \Big/ \left[a + k_T(T) + \Sigma \, k_s(S) \right] \quad (19)$$

It follows directly that:

$$G_i = (T)/1.0377 \times 10^{-9} \, D_{37} \quad (20)$$

This conventional approach suffers from two major problems: (a) The key rate constants k_T and k_T' are unknown for biological targets and frequently are estimated incorrectly as $k_T = 4\pi r_o D$, where r_o is the target radius and D is the radical diffusion constant. (b) The method is not easily extended to multi-hit kinetics. In connection with (a), it should be noted that the Smoluchowski result for diffusion-limited reactions is only valid when the target radius r_o is much smaller than the diffusion length of the radicals, which may be taken as

$$\rho = (D/a)^{\frac{1}{2}} \quad (21)$$

where $a(sec^{-1})$ is the radical decay rate constant.

An alternative approach based on target theory has been developed, by extending an analysis originally due to Hutchinson (1975) for primary radical attack

on spherical targets to include secondary radicals.

The average number of "hits" on the system after dose D can be expressed as:

$$\bar{n} = 6.25 \times 10^{11}\ D(\text{rads}) \left\{ 10^2 (v_d d_o / E_o) + G_R d \left[\eta_R v_R + \eta_{R'} v_{R'} \right] \right\} \qquad (22)$$

where v_d is the target volume (cm^3) for direct action, v_R and $v_{R'}$ are "reaction volumes" for the indirect attack of primary and secondary radicals, respectively, the η's are the corresponding damage efficiencies, E_o is the energy (ev) of a direct "hit", d_o and d are the mass densities of the direct action target and the medium, respectively. The dose-response curve for one-hit kinetics can be expressed as:

$$f = me^{-\bar{n}} \qquad (23)$$

where f is the surviving fraction and m is the "extrapolation number" for the high dose region of multi-target one-hit kinetics. (For pure exponential decay m = 1.) The linear slope of the $\log_e f$ *vs* D plot is given by:

$$- d(\log_e f)/dD = \bar{n}/D = 6.25 \times 10^{11}\ D \left\{ 10^2 (v_d / d_o / E_o) + G_R d \left[\eta_R v_R + \eta_{R'} v_{R'} \right] \right\}$$

providing a direct relationship between the dose-response data and the parameters of (22). It is convenient to define the radiation sensitivity as $1/D_o$, where D_o is the dose required for a 63% decrease in f on the linear region:

$$\underline{S} \equiv 1/D_o = 6.25 \times 10^{11} \left\{ 10^2 (v_D d_o / E_o) + G_R d \left[\eta_R v_R + \eta_{R'} v_{R'} \right] \right\} \qquad (24)$$

The G_i value for the indirect action component is given by:

$$G_i = C_T G_R \left[\eta_R v_R + \eta_{R'} v_{R'} \right] \qquad (25)$$

where C_T is the target concentration (cm^{-3}).

In applying the above formulation to experimental data, the η's are the key unknowns in (24) and (25) because the v's are fully determined by physical parameters. For the primary radicals, Hutchinson (1957) has shown that:

$$v_R = 4\pi r_o \rho^2 q(1 + r_o/\rho) \tag{26}$$

and

$$1/q = 1 + (4\pi r_o D/k)\ (1 + r_o/\rho) \tag{27}$$

in which k is the "true" rate constant at the surface of the target and the radical diffusion length ρ is defined by (21). For diffusion limited radical reactions $q \simeq 1$; otherwise only the product $q\eta$ can be determined since k is unknown. The above result is obtained by calculating the probability that a radical generated at r_1 from the center of the target can reach the surface in competition with scavenging: $P_{r_o}(r_1) = q(r_o/r_1)e^{-(r_1-r_o)/\rho}$. It follows immediately that: $v = \int_{r_o}^{\infty} 4\pi r_1^2 P_{r_o}(r_1) dr_1$.

This Hutchinson result is extended to secondary radicals generated by scavenging of R· by calculating the integral:

$$v_{R'} = \int_{r_o}^{\infty} 4\pi r_1^2\, dr_1 \int_{r_o}^{\infty} 4\pi r^2 g' P'_{r_o}(r)\ C_{r_1}(r)\, dr \tag{28}$$

where $P'_{r_o}(r)$ is the probability that the secondary radical generated at r reaches r_o, $C_{r_1}(r)$ is the normalized, steady-state concentration of secondary radicals at r generated by primary radicals formed at r_1 at a rate of one per second, and g' is the generation rate constant of secondary radicals (sec^{-1}). The detailed analysis (Becker et al., 1977) leads to:

$$v'_R = 4\pi r_o q'(\rho^2\rho'^2/D)g' \left[1 + \frac{r_o}{\rho+\rho'}\right] \tag{29}$$

where the primed terms apply to the secondary radicals and the un-primed terms to the primary radicals.

Substitution of (28) and (29) in (24), dropping the direct action term, and taking d = 1, gives:

$$\underline{S} = 6.25 \times 10^{11}\, G_R \rho^2 \left[\eta_R (4\pi r_o q)(1 + r_o/\rho) + \eta_{R'}\, (4\pi r_o q')\rho'^2 g'(1 + r_o/\rho+\rho') \right] \tag{30}$$

This result is equivalent to (19) for the case where the target separation is much longer than the radical diffusion length, i.e. $k_T(T) \ll a + \Sigma k_s(S)$ and $k'_T(T) \ll a'$. (Experimentally, this case obtains when the radiation sensitivity does not depend on the target concentration.) However, the key rate constants are now expressed explicitly as:

$$\begin{aligned} k_T &= 6.023 \times 10^{20}\, (4\pi r_o D)\, q(1 + r_o/\rho) \\ k'_T &= 6.023 \times 10^{20}\, (4\pi r_o D')q'(1 + r_o/\rho+\rho') \end{aligned} \tag{31}$$

For the case of small targets (i.e. $r_o \ll \rho, \rho'$), (31) reduces to the Smolukowski result. However, when the target dimensions are comparable to or larger than the radical diffusion lengths then $k_T \sim r_o^2 D^{\frac{1}{2}}$ even for the diffusion limited case ($q \simeq 1$).

Figure 15 shows the dependence of v_{OH} (left ordinate) in $k_s(S)$ for T7 phage taking standard values $G_{OH} = 2.7$, $D_{OH} = 2.3 \times 10^{-5}$ cm^2/sec and $r_o = 350$ Å. The OH decay rate constant was taken as 1.2×10^4 sec^{-1} based on the measurements of Becker et al. (1977) in 60 mM phosphate buffer at pH 7, where T7 phage was irradiated with 25 Mev electrons. The decrease of the OH reaction volume with increasing scavenger concentration is accompanied by the increase of the secondary radical target volume v'. This quantity was calculated for a secondary species with

Figure 15

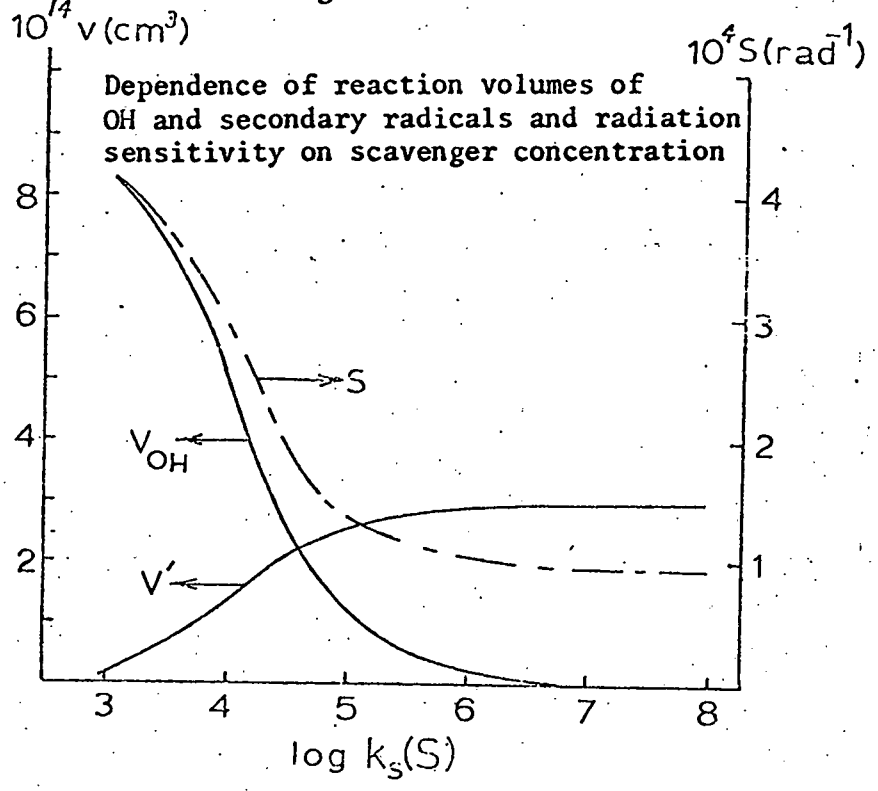
10^{14} v (cm^3)
10^4S(rad^{-1})
Dependence of reaction volumes of OH and secondary radicals and radiation sensitivity on scavenger concentration
S
V_{OH}
V'
log k_s(S)

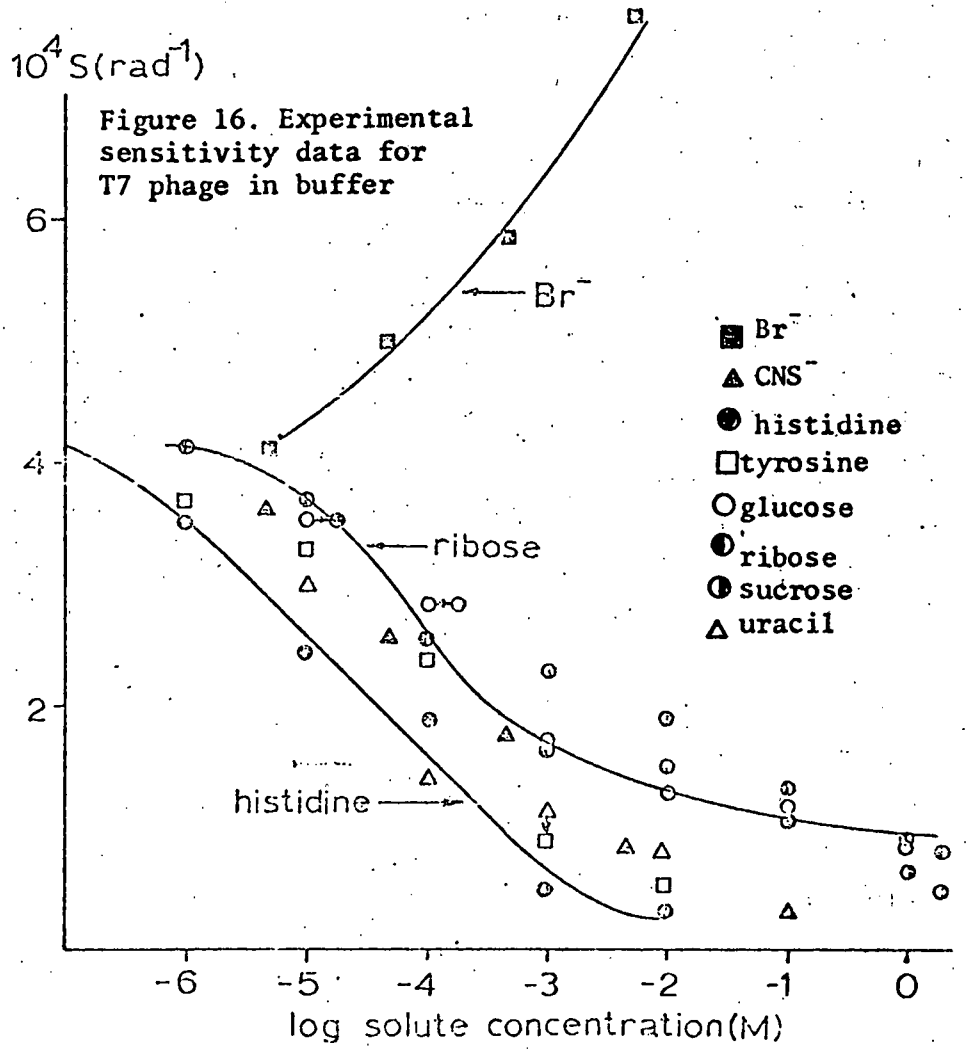
10^4S(rad^{-1})
Figure 16. Experimental sensitivity data for T7 phage in buffer
Br$^-$
ribose
histidine
Br$^-$
CNS$^-$
histidine
tyrosine
glucose
ribose
sucrose
uracil
log solute concentration(M)

$a' = 1 \times 10^4$ sec^{-1} and $D' = 0.6 \times 10^{-5}$ cm^2/sec. The right ordinate shows the corresponding radiation sensitivity ($1/D_{37}$) taking $q'\eta_{R'}/q_{OH}\eta_{OH} = 0.5$ as a typical value. Experimental results for irradiation of T7 phage in 60 mM buffer (plus 1 mM $MgSO_4$) in the presence of amino acids, sugars, and anions are given in Fig. 16. (This work was done at Michael Reese Hospital in collaboration with the present program.) With the exception of Br^- the general dependence on (S) follows the predictions. (The anomalously high sensitization by high Br^- may be due to the conversion of Br_2^- to Br_3^{2-} or anion binding to the phage at high Br^- concentrations.) Table V indicates the relative sensitizing ability of the various additives relative to OH radicals, where v' measures the ability of the secondary radical to reach the phage surface and $\eta_{R'}$ measures the inactivating efficiency at the surface. D_{37} leads to the product of these quantities as given in the last column of the table. The separation of η and v requires an independent determination of η_{OH} and information about a', the secondary radical decay rate. Based on the change of D_{37} with pulse dose, Becker et al. (1977) obtained $q_{OH}\eta_{OH} = 0.0027$ for T7 phage in phosphate buffer. In one set of measurements, T7 phage was irradiated in the presence of 90 mM Br^- to convert OH to Br_2^- and histidine was added to scavenge the Br_2^- (Fig. 17, open circles). The dashed line is the fit to (30) based on $D'(Br_2^-) = 0.6 \times 10^{-5}$ cm^2/sec from Stokes' law, $k(OH+Br^-) = 1.1 \times 10^9$ M^{-1}sec^{-1}, $k(Br_2^- + \text{histidine}) = 1.5 \times 10^7$ M^{-1} sec^{-1}, and the "best fit" parameters $q_{Br_2^-}\ \eta_{Br_2^-} = 0.0013$ and $a' = 450$ sec^{-1}. The results show that Br_2^- has a better chance of reaching the phage surface because of the longer lifetime than OH but is about half as effective for inactivating the phage at the surface. However, the overall effect is sensitizing relative to OH as expressed by the measured D_{37} values.

The same analysis can be applied to photodynamic action, where the triplet state of the external sensitizer is the "primary" radical and singlet oxygen (Δ)

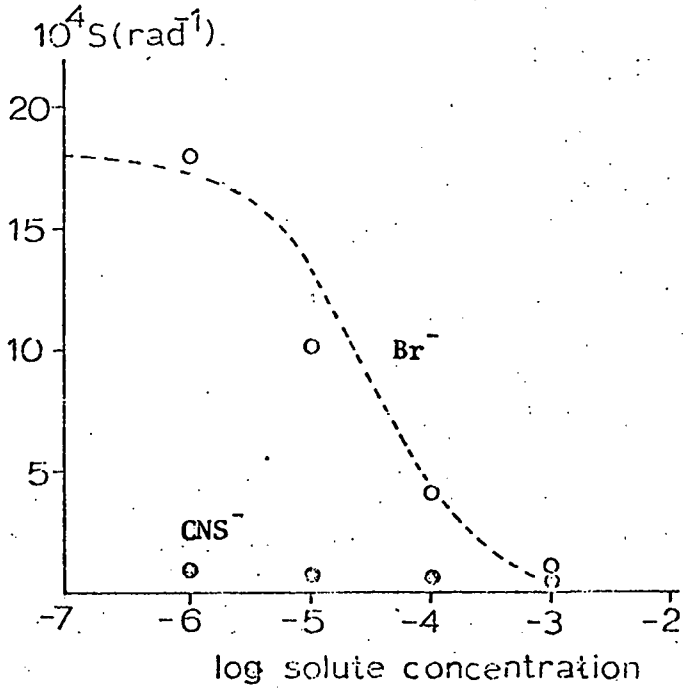

Figure 17. Protective action of histidine on T7 phage radiosensitization by 90 mM Br^- and 70 mM CNS^-. The dashed line is based on Eq. 30.

Solute	10^{-9} ks [a] (M^{-1} sec^{-1})	10^{6}/ks [b] (mM)	10^{4} S' [c] (rad^{-1})	$\eta'v'/\eta_{OH}v_{OH}$
Tyrosine	22	0.05	2.4	0.63
CNS^{-}	11	0.09	1.9	0.50
Uracil	7	0.14	1.0	0.26
Histidine	5	0.2	0.5	0.13
Sucrose	2.5	0.4	2.3	0.60
Ribose	2.1	0.5	1.5	0.39
Glucose	2	0.5	1.7	0.45
Br^{-}	1.1	0.9	6.1	1.61

(a) Rate constant for reaction with OH radicals.

(b) Minimum solute concentration for secondary radical dominance.

(c) Sensitivity to secondary radicals; N_2-sat 60 mM buffer.

Table V. Sensitivity of T7 Phage to Secondary Solute Radicals.

or O_2^- is the "secondary" radical. The equivalent to (24) for this case is:

$$1/D_{37} = \phi_T^o \, (\eta_T v_T + \eta_\Delta v_\Delta) \tag{32}$$

where ϕ_T^o is the intersystem crossing efficiency of the sensitizer. The corresponding quantum yield of the observable effect is:

$$\phi_i = C_T/D_{37} \tag{33}$$

where the dose is in units of quanta/cm^3.

A typical application to the data of Cohn and Tseng (1977) on the photodynamic inactivation of Saccharomyces cerevisiae sensitized by eosin Y illustrates the utility of the method. The semilogarithmic survival curves are linear in the high-dose region with an initial shoulder. The results with 10 μM dye led to $D_o(N_2) = 2.0$ and $D_o(O_2) = 0.5$ on a relative dose scale. The enhancement of ϕ_i in D_2O and protection by azide (Cohn et al., 1977) indicate that Δ is the dominant secondary species. Accordingly, direct substitutions in (32) lead to $\eta_\Delta/\eta_T = 25$ with appropriate values of the v's from (26) and (29). [In calculating the v's it was assumed that $q = q' = 1$; $r_o = 2.5$ microns; $\rho_T^2 = D_T/\left[k_{T+S}(S) + k_{T+O_2}(O_2)\right]$ $\rho_\Delta^2 = D_\Delta \tau_\Delta$; $g' = p_\Delta k_{T+O_2}$, where all quantities for eosin Y and oxygen are known or can be estimated accurately; see Grossweiner (1977). It is found that $v_T = 29 \times 10^{-12}$ cm^3 in N_2 and $v_T = 1.4 \times 10^{-12}$ cm^3 and $v_\Delta = 4.6 \times 10^{-12}$ cm^3 in O_2.] The inactivation quantum yield on the high dose region was 1.2×10^{-13} at an active yeast concentration of $8 \times 10^5/cm^3$. Taking $\phi_T^o = 0.64$, (32) and (33) give $\eta_\Delta = 5 \times 10^{-8}$ and the product of η_Δ and the yeast surface area $4\pi r_o^2$ gives 400 A^2 as the size of the sensitive target. It may be concluded that a target comparable to the dimensions of a protein molecule remains available for one-hit inactivation by singlet oxygen after saturation of the low-dose, multi-target regime where the sub-lethal damage occurs.

4. Photosensitization by Psoralens

The clinical applications of psoralen derivatives in connection with phototherapy of psoriasis and vitiligo has led to considerable interest in the mechanism of their photosensitizing properties. It is generally accepted that psoralen derivatives form monofunctional and bi-functional photoadducts with DNA pyrimidine bases (e.g. Musajo and Rodighiero, 1972; Pathak et al., 1974; Musajo et al., 1974) although the specific relationship of the photochemical products to the biological effects has not been explained. Recent work from this laboratory (Poppe and Grossweiner, 1975) deomonstrated that 8-methoxypsoralen (8-MOP) photosensitizes the inactivation of hen lysozyme and the oxidation of I^-, and that singlet oxygen (Δ) is the major damaging intermediate. This result is surprising because the previous work indicates that the cellular DNA damage does not involve oxygen. However, we found that the presence of poly (dA-dT) inhibits the photooxidizing reactions, suggesting that the dark binding of 8-MOP to the substrate promotes the Type I pathway. These findings are relevant to the clinical applications of psoralens as well, because Δ is a labile species damaging to proteins and membranes and might be involved in the undesirable side effects of the phototherapeutic procedures. The preliminary studies on photosensitization by 8-MOP has been extended in new work to obtain additional information about the initial photosensitizing mechanisms.

Electronic Excitation of 8-Methoxypsoralen

a) Fluorescence. The fluorescence emission of 8-MOP in H_2O measured with a Perkin-Elmer Model 204 Fluorescence Spectrophotometer shows a major band at 495 nm (uncorrected) with a weak band at 615 nm for 311 nm excitation. A new band appears in water-glycerole solutions near 380 nm reaching the maximum intensity in 100% glycerole. The fluorescence lifetimes were measured with a PRA Model 510 repetitive flash lamp providing 3.5 nsec pulses from an air discharge. The signal was detected with a 1P28 photomultiplier and measured with a PAR Model 162 Boxcar Averager.

The lifetime analysis was carried out with a deconvolution method based on "least squares" using a PDP 11/45 digital computer located at Michael Reese Medical Center. The results obtained by exciting 8-MOP through a Corning CS No. 7-54 filter (204 - 400 nm) and measuring the emission through a CS No. 3-72 filter (>450 nm) are: H_2O - 1.4 nsec (1.9 nsec); 60% glycerole-H_2O - 2.4 nsec; 100% glycerole - 2.6 nsec (2.5) where the results in parenthesis were reported in preliminary work of Poppe and Grossweiner (1975).

In view of the interest in the effect of substrate binding on the photochemical mechanisms of psoralens, the fluorescence efficiency was measured in water-glycerole solutions of varying viscosity. The results in Table VI show a marked increase of fluorescence efficiency with viscosity, suggesting that molecular rigidity may promote population of the excited singlet and triplet states.

Table VI. Dependence of 8-MOP Fluorescence Efficiency on Viscosity on Water-Glycerole Solutions

Wt % glycerole	viscosity (CP)	ϕ_{fl}(rel)*
8.7	1.3	0.01
20	1.8	0.089
35	3.1	0.165
40	3.7	0.205
50	6.0	0.36
60	10.8	0.267
70	22.5	0.43
80	60.1	0.49
90	219	0.51

*excited 302 nm; measured 350 nm

b) Flash Photolysis Studies on 8-MOP. In preliminary work, Poppe and Grossweiner (1975) reported that flash irradiation of 8-MOP (> 305 nm) generates a broad, visible absorption with poorly resolved peaks near 600 nm, 480 nm and <360 nm. The decay lifetime was about 200 μsec in glycerole and 1.8 μsec in in H_2O. The transient product was attributed to the 8-MOP triplet state based on the exponential decay and quenching by oxygen at $kq \simeq 1 \times 10^9$. Indirect evidence indicates that the 8-MOP triplet state is involved in the C4-cycloaddition to pyrimidine bases in DNA, based on luminescence spectra (Pathak et al., 1961; Mantulin and Song, 1973), molecular orbital calculations (Song et al., 1971), zero-field splitting parameters (Moore et al., 1976) and photochemical studies (Bevilacqua and Bordin, 1973; Gervais and Schryver, 1975). A more definitive identification of the flash photolysis transient has been made by generating the same transient absorption with triplet energy transfer. Based on the estimated triplet energy of 8-MOP of 61.7 kcal/mole (Gervais and Schryver, 1975) from phosphorescence spectra, possible donors are benzophenone (E_T = 69.3 kcal/mole) and acetophenone (E_T=73.6 kcal/mole). In one set of experiments, 6 mM benzophenone was irradiated in benzene containing 0.026 M ethanol with and without 25 μM 8-MOP. (These conditions were selected to minimize direct light absorption by 8-MOP.) The transient spectra at 100 μsec delay showed the benzophenone ketyl radical at 520 and 545 nm and an additional absorption when 8-MOP was present which is attributed to the triplet state. A more definite result was obtained with acetophenone sensitization where irradiation of 0.02 M in benzene with 2 M ethanol gives the ketyl radical (Fig. 18) and the addition of 25 μM 8-MOP leads to significantly higher overall absorption with peaks near 500 nm and 600 nm. The lowest line shows the triplet spectrum obtained by direct irradiation of 75 μM 8-MOP (3X higher) without acetophenone for comparison.

The above experiments were done with the xenon flash system and photographic plate detection. Laser flash experiments with 8-MOP in water (Fig. 19) generates

Figure 18. Photosensitized formation of triplet 8-MOP by acetophenone in benzene with 2M ethanol; irradiated at $\lambda > 305$ nm

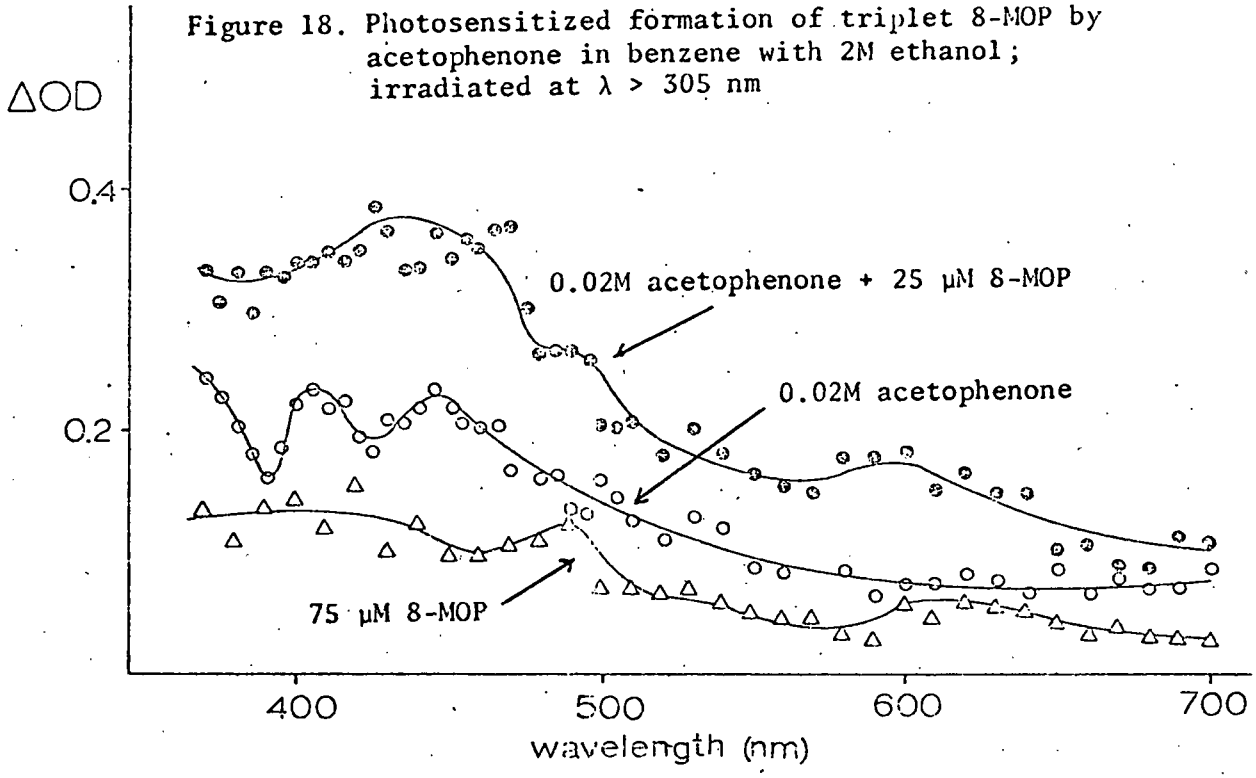

Figure 19, Laser photolysis of 135 μM 8-MOP in water(265 nm)

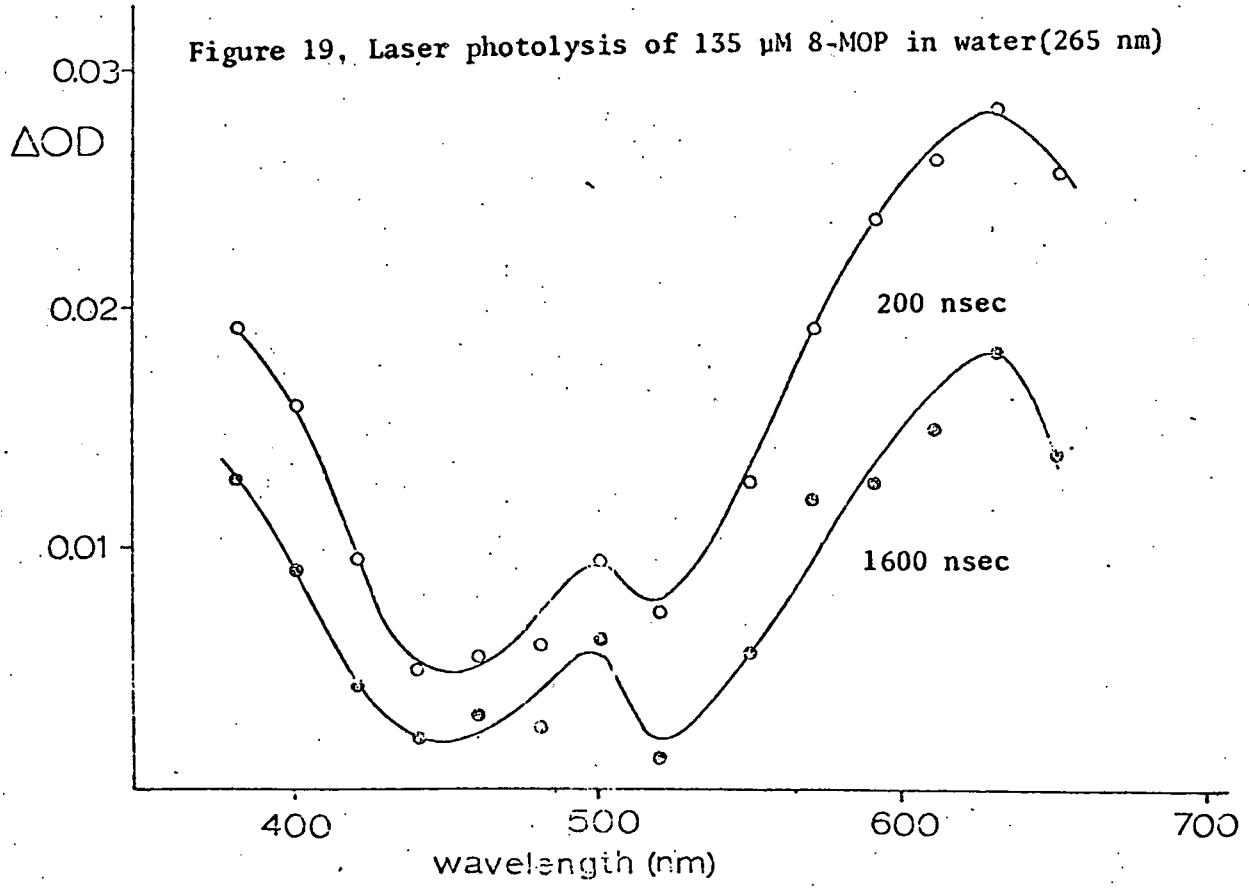

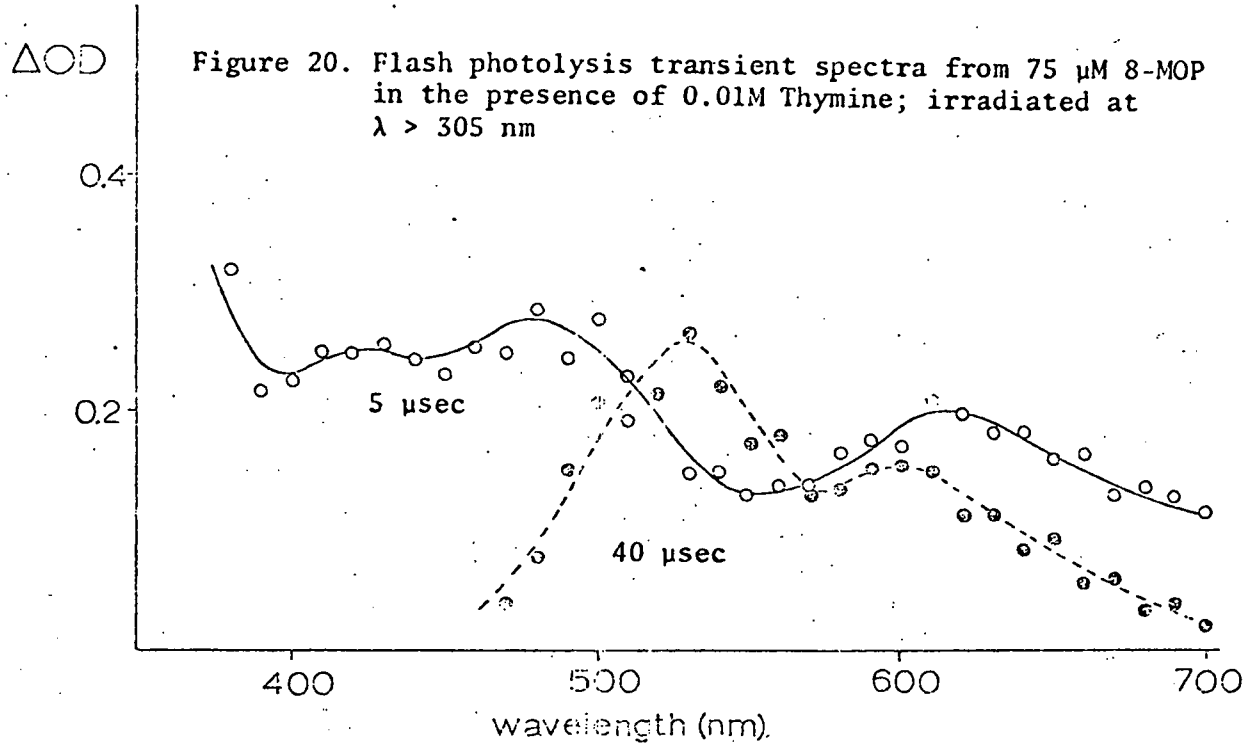

Figure 20. Flash photolysis transient spectra from 75 μM 8-MOP in the presence of 0.01M Thymine; irradiated at $\lambda > 305$ nm

a well-resolved triplet spectrum in water. Decay measurements in 80% glycerole-water, to slow down the decay rate, led to a first-order decay lifetime of 210 ± 35 μsec at 380 nm, 480 nm, and 590 nm indicating that a single product is formed. It should be noted, however, that Land (1977) reported an 8-MOP triplet absorption obtained by pulse radiolysis in benzene that does not show the 600 nm band, a discrepancy that must be resolved.

In current work, 8-MOP is being irradiated in the presence of thymine to determine the initial photochemical reactions invovled in photoadduct formation. The results in Fig. 20 indicate that triplet 8-MOP reacts with thymine to form a new product with absorption bands at 530 nm and near 600 nm. Land (1977) reported a rate constant for the case of psoralen of 7.5×10^8 $\underline{M}^{-1}sec^{-1}$ but the reaction may be slower for 8-MOP, $\sim 10^7$ $\underline{M}^{-1}sec^{-1}$ based on our preliminary data. This work is in progress and will be extended to other DNA bases, polynucleotides and DNA.

c) Photosensitized Inactivation of Hen Lysozyme

Poppe and Grossweiner (1975) reported that 8-MOP photosensitizes the inactivation of hen lysozyme to near-UV irradiation. The importance of singlet oxygen (Δ) was demonstrated by protection with added azide ion and the enhanced inactivation quantum yield in D_2O. Furthermore, the dependence of ϕ_{in} on the initial lysozyme concentration led to the rate constant $k(L + \Delta) = 1.3 \times 10^9$ $\underline{M}^{-1}$ sec^{-1} in agreement with 1.9×10^9 reported by Kepka and Grossweiner (1973) for eosin sensitization and 1.5×10^9 obtained by Matheson et al., (1975) where Δ was generated directly with a Nd-YAG laser. The continuation of this work indicates that the 8-MOP/lysozyme system is more complicated than originally believed, although the major role of Δ is strongly supported. In contrast to I^- as the acceptor of Δ, the sensitizing action of 8-MOP is only important in D_2O/O_2 systems, as evidenced by the representative inactivation quantum yields data below:

	with 8-MOP (200 μM)		without 8-MOP	
	N_2	O_2	N_2	O_2
H_2O	0.4	2.2	0.4	1.5
D_2O	3.1	25	0.8	1.2

The smaller changes with irradiation conditions probably are related to hydrogen exchange, impurity sensitization, direct absorption by lysozyme in the near-UV region, etc., which have not been explored in detail. In order to evaluate the Δ contribution, histidine was added as a competitive acceptor, based on $k(\Delta + His) = 1.7 \times 10^8\ \underline{M}^{-1}\ sec^{-1}$ (Matheson *et al.*, 1975). The results in Fig. 21 show that protection of 2.7 μM lysozyme in the presence of 200 μM 8-MOP (D_2O/O_2) takes place at (His) $\sim 10^{-5}$ M, much too low to be explained by bulk reactions. Furthermore, the extent of protection saturates and becomes less effective at (His) $\sim 10^{-3}$ M.

A possible explanation for the unexpected results involves the binding of 8-MOP to the enzyme, a situation previously encountered in connection with the eosin/lysozyme system (Kepka and Grossweiner, 1973). If this is the case, protection at low histidine concentrations may result from competition for the key binding site between 8-MOP and histidine, while the subsequent enhanced photosensitivity at higher histidine concentrations can be explained by bulk reactions of Δ with 8-MOP and the formation of toxic products. Independent support of this mechanism derives from the dependence of the lysozyme inactivation rate on lysozyme concentration. Data for the slope of the semilogarithmic enzyme activity *vs* time plot (200μM 8-MOP, D_2O/O_2):

(Lys) μM	1.1	1.6	2.2	2.7
Activity (min^{-1})	0.034	0.022	0.019	0.015

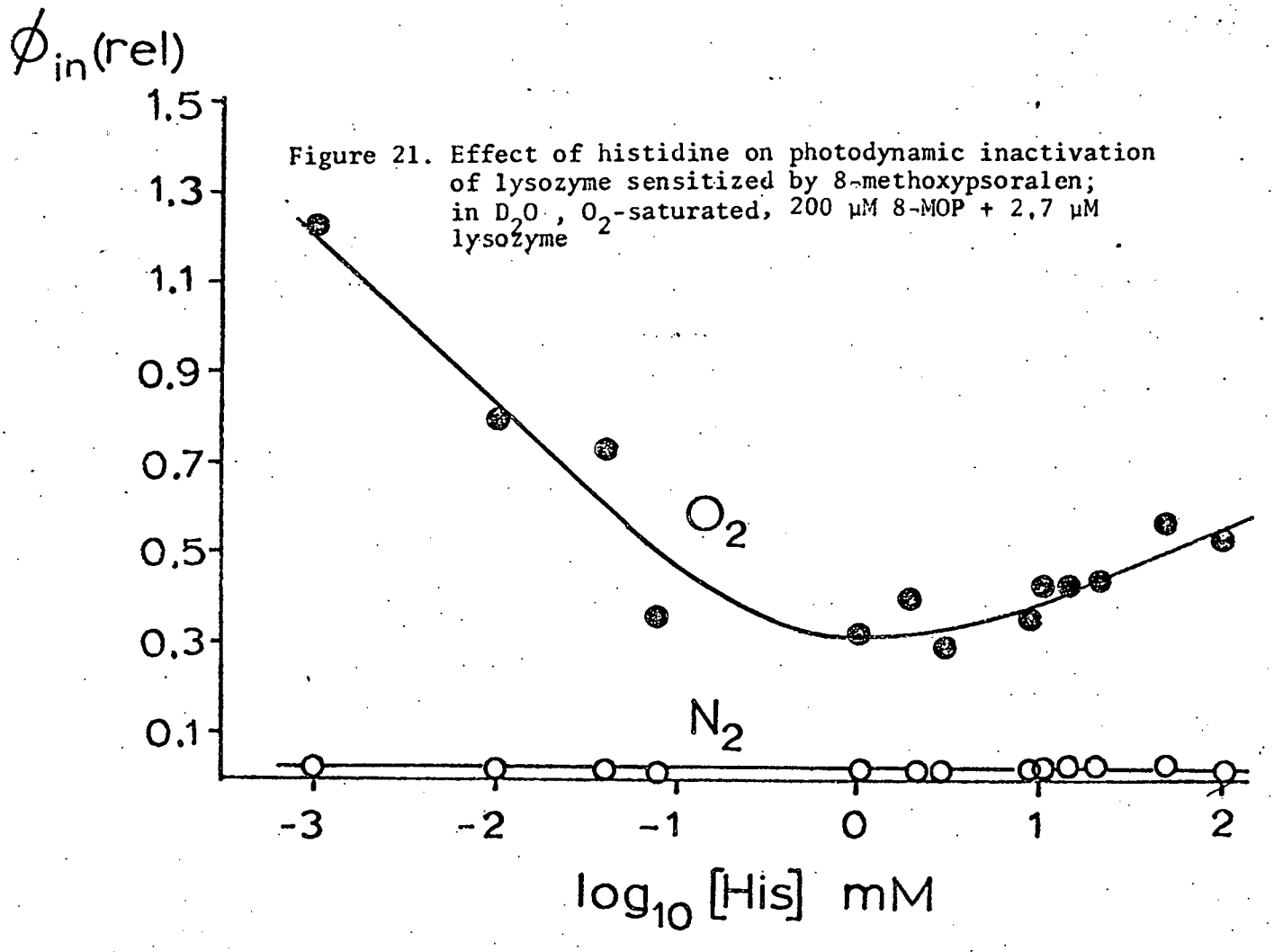

Figure 21. Effect of histidine on photodynamic inactivation of lysozyme sensitized by 8-methoxypsoralen; in D_2O, O_2-saturated, 200 µM 8-MOP + 2,7 µM lysozyme

lead to $k(L + \Delta) \sim 1 \times 10^{11}$ $\underline{M}^{-1}$ sec^{-1} if bulk reactions are involved, an unrealistically high result. However, the same data are consistent with usual binding constants if the complexing of 8-MOP to the enzyme strongly sensitizes the enzyme to the attack of Δ, as shown to be the case for eosin, where the binding site was identified with essential Trp 108 on the enzyme surface. The complexing of psoralens to protein is of evident importance in conjunction with the phototherapeutic applications, particularly where singlet oxygen is a key photoproduct. This photochemical study is being continued in current work and will be extended to binding studies based on fluorescent techniques in new work.

5. Radiosensitization by Psoralens

Anoxic sensitization of T7 bacteriophage by 8-MOP was reported recently in a collaborative investigation with Michael Reese Medical Center (Becker et al., 1975). In view of the great interest in anoxic sensitizers in connection with radiation therapy of cancer, the preliminary work has been extended in order to obtain additional information about the mechanism and generality of the effect for other psoralen derivatives.

The experiments were carried out by irradiating T7 phage suspensions in 100 mM histidine or in nutrient broth (NB) under conditions where solvent radicals generated in the external medium are effectively scavenged. The survival curves were accurately exponential and independent of phage titre from 10^4 to 10^8 per cm^3. The irradiations were performed with 1 μsec pulses of 25 Mev electrons at a typical pulse dose of 1 rad/pulse and the phage activity was assayed by means of placque formation on E. coli B/r. The other experimental details are available in the Ph.D. Thesis of D. Becker (Illinois Institute of Technology, May 1977) and in Becker et al., (1977).

The results in Table VI show that 8-MOP enhances the radiation sensitivity S ($1/D_{37}$) by a factor of 3 in anoxic NB but not with O_2 saturation. There is ample evidence that oxygen promotes single strand breaks (ssb) and double strand breaks (dsb) in phage DNA including T7; e.g. Blok and Loman (1973). These authors suggested that O_2 blocks a non-strand break lesion (nsb) proposed as cross links (cl). Accordingly, it is reasonable to postulate that the bifunctional agent 8-MOP promotes the cl damage component and that this process is inhibited by oxygen. The protection of T7 by dithiothreitol (DTT) is consistent with other sulfydryl agents. However, the combined action of 8-MOP and DTT leads to higher sensitivity in O_2, a surprising "oxygen effect" in phage which usually is not affected by oxygen or is less sensitive.

The relationship between the DNA lesions and phage inactivation has been the subject of much recent work. In a study of PM2 phage circular, double-stranded

Medium	Additive(s)	10^4 S (rad^{-1}) N_2	O_2
Nutrient Broth [a]	-	0.078	0.068
Nutrient Broth	0.3 mM 8-MOP [b]	0.20	0.068
Nutrient Broth	25 mM DTT [c]	0.028	0.063
Nutrient Broth	0.3 mM 8-MOP + 25 mM DTT	0.055	0.11
100 mM Histidine	-	0.32	0.33
100 mM Histidine	N_2O	0.32	
100 mM Histidine	25 mM DTT	0.17	
100 mM Histidine	0.3 mM 8-MOP	0.74	0.36
100 mM Histidine	0.03 mM 5-MOP [d]	0.63	0.35
100 mM Histidine	0.03 mM TMP [e]	0.83	0.30
100 mM Histidine	0.3 mM DHP [f]	0.56	0.33

(a) 8 gl Difco Bacto Nutrient Broth
(b) 8-methoxypsoralen
(c) dithiothreitol
(d) 5-methoxypsoralen
(e) 4,5',8-trimethylpsoralen
(f) 5,8-dihydroxypsoralen

Table VI. Radiation Sensitivity of T7 Phage in Protective Conditions

DNA, Van der Schans et al. (1973) assumed that the various damage types contribute independently to inactivation and deduced that the relative contributions of ssb, dsb and n are 8.5%, 4.5% and 87% respectively. The corresponding inactivation efficiencies per lesion were $f_{ssb} = 0.02$, $f_{dsb} = 1.00$ and $f_n = 0.28f_n^s$, where f_n^s is the inactivation efficiency of a nucleotide alteration in single-stranded PM2 DNA. In these experiments the extracted DNA was irradiated with ^{60}Co in O_2-sat, dilute aqueous solutions. Similar measurements of Van der Schans and Bleichrodt (1974) carried out in NB at -196°C led to: $f_{ssb} = 0.02$, $f_{dsb} = 1$, and $f_n = 0.13f_n^s$. These results provide good evidence for the high lethality of dsb and low lethality of ssb under conditions of direct and indirect action, but cannot be extended to non-strand break damage in the intact phage. The recent work of Hawkins (1976) on T7 indicates that covalent, DNA-protein cross links are formed by ^{60}Co irradiations in aerobic buffer with 1 mM histidine. Since this medium scavenges external radicals (Fig. 16) it can be concluded that radiolysis of internal water and/or direct action promote cross links.

The G values for inactivation and strand breaks in T7 phage irradiated with ^{60}Co in protective conditions reported by Blok and Loman (1973) are summarized in Table VII. [The damage yields per 100 ev absorbed by the phage DNA are related to the S values by: $G_{in} = 9.637 \times 10^{11}\ S(rad^{-1})/MW\ (daltons)$.] Since G_{ssb} and G_{dsb} are 1.4 and 2.7 times higher in O_2, respectively, nucleotide damage or another non-strand break lesion must be strongly inhibited by O_2. The general approach of Van der Schans et al. (1973) has been employed by assuming additivity of damage contributions: $G_{in} = f_{ssb}G_{ssb} + f_{dsb}G_{dsb} + f_{nsb}G_{nsb}$, where the last term refers to non-strand break damage of any type including cross links. In order to estimate the contribution of nsb damage it is assumed: (a) $f_{dsb} = 1$ and (b) $g_{nsb} = 0$ in oxygenated protective media without other additives. The data in the first two rows of Table VII lead immediately to: $f_{ssb} = 0.13$. When these results are applied to the data in rows 3 and 4 it is found that $(fG)_{nsb} = -0.03$ and $(fG)_{nsb} = 0.00$,

1	2	3	4	5	6	7
Condition	G_{in} (a)	this work (b)	G_{ssb}/G_{in} (c)	G_{dsb}/G_{in} (c)	$(Gf)_{nsb}$ (d)	$(Gf)_{nsb}/G_{in}$ (e)
N_2	0.39	0.30	3	0.10	0.19	0.5
O_2	0.32	0.26	5	0.33	0	0
N_2 + 0.15 M + thioglycol	0.097	0.11 (f)	7	0.40	0.0	0
O_2 + 0.15 M + thioglycol	0.22	0.24 (f)	5	0.32	0.0	0
N_2 + 0.3 mM + 8-MOP	-	0.77	-		0.47	0.6
O_2 + 0.3 mM	-	0.26	-		0.0	0
N_2 + 0.3 mM + 8-MOP + 25 mM DTT	-	0.21	-		0.11	0.5
O_2 + 0.3 mM + 8-MOP + 25 mM DTT	-	0.42	-		0.20	0.5

(a) Phage inactivated per 100 ev absorbed in DNA; from Blok and Loman (1973); in 0.1 M thiourea.

(b) in 1X nutrient broth

(c) Strand breaks per phage inactivated; from Blok and Loman (1973)

(d) Calculated yield of non-strand break damage per 100 ev based on $f_{ssb} = 0.13$ and $f_{dsb} = 1$.

(e) Fractional contribution of non-strand break damage to inactivation yeilds

(f) with 25 mM DTT

Table VII. Inactivation and DNA Damage Yields in T7 Phage Irradiated in Protective Media

respectively, for anoxic and oxygeneated solutions with high thioglycol or in nutrient broth.

The analysis supports the conclusion that non-strand break damage is strongly inhibited by either oxygen or high sulfhydryl in the presence of effective radical scavengers. The maximum contribution of nsb lesions to inactivation is estimated in columns 6 and 7 assuming that the presence of 8-MOP does not enhance the yields of strand breaks. The results in the last column indicate that 8-MOP promotes the formation of nsb damage by a factor of 2.5 in anoxic conditions. However, the sensitizing action of 8-MOP is equivalent to nitrogen alone when both oxygen and sulfhydryl are present, leading to a nsb contribution the same as anoxic phage in NB. These considerations strongly suggest the psoralens act as cross-linking agents probably promoting covalent bonds between the phage DNA and protein. The inhibiting effect of oxygen on cross link formation has been observed previously for irradiation of dry DNA (Alexander and Lett, 1960) and moist DNA (Hagen and Wallstein, 1965) and may involve blocking of the primary radical site by perioxidation. The particularly high lethality of DNA-protein cross links for intact phage can be attributed to inhibition of DNA injection.

The chemical basis of 8-MOP sensitization has been clarified by recent pulse radiolysis studies on aqueous solutions of 8-MOP in the presence of nucleic acid bases. The rate constants for the initial reactions of e^-_{aq} or OH with 8-MOP are 1.0×10^{10} and 1.1×10^{10} $\underline{M}^{-1}$ sec^{-1}, respectively. Electron transfer experiments were carried out in which the nucleic acid base was irradiated with 25 MeV electrons in the presence of 8-MOP, under conditions that either e^-_{aq} or OH reacted first with the base. It was found that the electron adducts of thymine, uracil, cytosine and adenine transfer the extra electron to 8-MOP with 100% efficiency at rate constants $\sim 4 \times 10^9$ $\underline{M}^{-1}$ sec^{-1};

$$BH^- + 8\text{-MOP} \longrightarrow BH + 8\text{-MOP}^- \quad .$$

However, in the corresponding reactions of the base OH adducts double-bond ring addition products in the case of pyrimidines (Myers et al., 1968) molecular complex formation (VI) was found to be about three times more frequent than electron transfer to 8-MOP (VII):

$$\dot{B}H(OH) + 8\text{-MOP} \begin{cases} \nearrow BH(OH)\text{-}(8\text{-MOP})\cdot & \text{(VI)} \\ \searrow BH(OH)_2 + 8\text{-MOP}^- + H^+ & \text{(VII)} \end{cases}$$

Reaction (VI) may be the first step of 8-MOP cross link formation in protective media, followed by the subsequent reaction of the complex with a protein lesion. The blocking of (VI) by oxygen or sulfhydryl is consistent with this mechanism:

$$\dot{B}H(OH) + O_2 \longrightarrow BH(OH)\text{—}O_2\cdot \qquad \text{(VIII)}$$

$$\dot{B}H(OH) + RSH \longrightarrow BH(OH)(H_2) + RS\cdot \qquad \text{(IX)}$$

where $BH(OH)\text{—}O_2\cdot$ is the hydroperoxy radical of the hydroxylated base and $BH(OH)(H_2)$ is the hydroxydihydro derivative of the base. The high contribution of cross links to inactivation when 8-MOP is present with both O_2 and SH (Table VI) can be explained by several possible mechanisms. For example, the hydroxyperoxy radical of (VIII) might be reduced by SH to O_2^- and BH(OH), which in turn reacts with 8-MOP localized by pre-irradiation bidding.

The results in 100 mM histidine (Table VI) differ from NB in that the sensitivities are about 3 times higher, indicative of contributions from secondary histidine radicals and possibly the radiolysis of internal water. (The insensitivity to O_2 and N_2O indicates that e^-_{aq} and OH from external water are not involved.) Several psoralen derivatives including 8-MOP are anoxic sensitizers in 100 mM histidine including 5,8-dihydroxypsoralen which is not a skin photosensitizer.

6. Photodynamic and Photosensitized Inactivation of Saccharomyces cerevisiae*

The biological effects of photodynamic action are being investigated in yeast cells with emphasis on damage to cell membranes in vivo. Yeast provides a particularly advantageous system for these studies since the organism multiplies rapidly and can be cultured on relatively simple media. The osmotic stability provided by the cell wall allows yeast to be suspended in water rather than a nutrient medium for irradiation, so that no inadvertent potential sensitizers from either growth medium or buffers are present. In addition, yeast is a eukaryotic micro-organism, so that the results may provide the basis for understanding of photoirradiation damage in higher eukaryotes.

Previous results have demonstrated that eosin Y remains in solution outside the cell where it can sensitize damage to the plasma membrane and that eosin is not toxic and does not affect the normal rate of cell multiplication (see Progress Report, 7/1/74-6/31/75). Irradiation in the presence of eosin and molecular oxygen results in a substantial decrease in cell survival which depends logarithmically on the dose at higher doses but which exhibits a low-dose shoulder. Anaerobic irradiation in the presence of eosin results in only a small degree of killing, while irradiation of an oxygen-saturated suspension in the absence of eosin causes no detectable killing. These results demonstrate that both eosin and molecular oxygen are required for the inactivation of yeast by visible light and that neither endogenous sensitizers nor toxicity of the dye is involved (see Progress Report, 7/1/75-6/30/76).

a) Kinetics and $^1O_2$ Mechanism of Eosin-sensitized Yeast Photoinactivation

Survival curves were obtained by irradiating strain Y55 diploid yeast with visible light ($\lambda > 400$) in the presence of oxygen and eosin Y. The cells were washed twice with distilled water and were resuspended in sterile aqueous eosin for irraidation. Prrallel measurements for irradiation of nitrogen-saturated yeast suspensions in the presence of eosin showed a marked reduction in the degree of cell inactivation. Survival curve parameters are summarized in Table VIII.

Eosin Concentration (μM)	Temperature (°C)	Saturating Gas	$D_o \times 10^{-9}$ (erg/cm^2) (400-550 nm)	Relative Sensitivity	Extrapolation Number (m)
5	27	O_2	30.9	0.060	1.0
5	30	O_2	4.44	0.419	1.6
10	30	O_2	1.86	1.00	3.3
2	30	N_2	15.1	0.124	1.1
10	30	N_2	7.17	0.260	1.3

Table VIII. Relative Sensitivity of Y55 Yeast to Eosin-Sensitized Photokilling

These results show that inactivation is caused primarily by eosin-sensitized photodynamic attack, although some degree of anoxic sensitization may be involved. Since eosin Y has been identified as an extracellular sensitizer, the plasma membrane must be considered as a possible primary target for the damaging agents which eosin generates (Cohn and Tseng, 1977).

Correction of Survival Curves for Eosin Bleaching

Irradiation of aqueous eosin solutions in the presence of oxygen causes photooxidative bleaching of the dye at a rate which depends on the oxygen concentration (Imamura, 1956; Usi et al., 1965). Bleaching rates were determined for eosin Y in aqueous solution by measuring the decrease in optical density at 515 nm as a function of irradiation time. The results obey the formula:

$$c(t) = c_o e^{-k_E t} \tag{34}$$

with $k_E = 0.0136\ \text{min}^{-1}$ for the eosin concentrations of interest, where c_o is the initial dye concentration and c(t) is the concentration at a later time t. The decrease in the concentration of active eosin caused by bleaching would cause the absorbed radiation dose to decrease with time. The fractional absorption during the course of the irradiation is given by:

$$A(t) = 1 - e^{-2.303(OD_o)e^{-k_E t}}$$

Multiplying this expression by the incident intensity, I(t) and the beam cross sectional area (a) and integrating over time gives the effective absorbed radiation dose D(t):

$$D(t) = \int_0^t I(t')\ a\ (1 - e^{-2.303(OD_o)e^{-k_E t'}})\ dt' \quad .$$

The effective exposure time is:

$$T(t) = \frac{D(t)}{I_o a} = \int_o^t (1 - e^{-2.303()D_o)} e^{-k_E t}) \, dt' \quad . \tag{35}$$

where T(t) is the exposure time which would be required to obtain the measured value of $N(t)/N_o$ in the absence of dye bleaching.

The integral for T(t) was evaluated by expanding the term $e^{-2.303(OD_o)e^{-k_E t'}}$ leading to:

$$T(t) = \frac{1}{k_E} \sum_{n=1}^{\infty} (-1)^{n+1} \frac{(2.303(OD)_o))^n}{n \cdot n!} (1 - e^{-nk_E t}) \quad . \tag{36}$$

The corrected surviving fractions for the photodynamic inactivation of yeast by 5 and 10 μM eosin at 30° follow a single curve which exhibits a low dose shoulder and an exponential decrease at higher dose (Cohn and Tseng, 1977).

Quantum Yield Calculations for Cell Inactivation

The quantum yields ϕ were calculated from survival curves with the following expression (Glad and Spikes, 1966):

$$\phi = \lim_{D \to o} \left[\frac{N(t)}{D(t)} \right] \simeq \frac{N_o / t_{37}}{(dQ/dt)_{t=0}} \tag{37}$$

where $(dQ/dt)_{t=0}$ is the initial rate of light absorption, t_{37} is the time at which 37% of the original cells still survive and n_o is the original number of cells. The incident intensity is given by:

$$P_{inc} = \int_{\lambda_1}^{\lambda_2} I_\lambda a d\lambda = \int_{\lambda_1}^{\lambda_2} n_\lambda h \frac{c}{\lambda} d\lambda,$$

where n_λ is the number of incident photons per unit wavelength interval per unit time. The emission intensity of the h.p. mercury-xenon arc is approximately

constant over the wavelength range 400 nm- 550 nm except for two sharp peaks at 438 nm and 546 nm. However, eosin absorbs weakly outside the wavelength region 500 nm - 530 nm and the total number of photons, N, incident on the sample per unit time can be obtained by integrating:

$$N = \int_{\lambda_1}^{\lambda_2} n_\lambda d\lambda = \frac{aI_\lambda \Delta\lambda}{2hc\Delta\lambda} (\lambda_2^2 - \lambda_1^2) \quad (38)$$

where λ_2 = 530 nm, λ_1 = 500 nm and $\Delta\lambda = \lambda_2 - \lambda_1$ = 30 nm. The incident intensity was measured as 1.0 x 10^6 erg/cm^2-sec for the interval 400-500 nm, so $I = I_\lambda \Delta\lambda$ = 2.0 x 10^5 ergs/cm^2. Substituting the numerical values and using a = 3.0 cm^2 gives N = 1.6 x 10^{17} photon/sec.

The results labeled "uncorrected quantum yield" in Table IX were obtained by using the measured incident dose to determine the number of incident photons, but this overestimates the actual dose (Jagger, 1967) because extracellular eosin Y attenuates the beam as it passes through the sample cuvette, and absorption by cell components could further attenuate the beam. Corrections to the incident dose for the absorption of light by eosin have been determined from the published tables, assuming that dose decreases exponentially with penetration distance into the sample and ignoring light scattering (Morowitz, 1950). Corrected values of ϕ are presented in the last two entires of Table IX.

The inactivation of quantum yields can be related to molecular parameters using competition kinetics:

$$\phi = \eta_\Delta \phi_T^o \gamma_\Delta \frac{k_T(\text{yeast})}{1/\tau_\Delta + k_T(\text{yeast})} \quad (39)$$

where ϕ_T^o = 0.64 is the intersystem crossing probability, γ_Δ = 0.89 is the efficiency that the reaction of triplet eosin with oxygen leads to singlet

Concentration of Eosin Y (μM)	5.0	10.0
t_{37} (sec)[(a)]	6840	4320
fractional absorption	0.669	0.890
uncorrected quantum yield	3.34×10^{-14}	3.99×10^{-14}
Morowitz correction factor	0.46	0.30
corrected quantum yield	7.3×10^{-14}	1.3×10^{-13}

(a) $N_o = 2.38 \times 10^7/cm^3$

Table IX. Quantum Yield Calculations for Eosin-Sensitized Photodynamic Inactivation of Yeast

oxygen (Usui, 1973), η_Δ is the inactivating efficiency of Δ and τ_Δ = 2 μsec is the decay lifetime of Δ in water. The results in Table IX lead to η_Δ = 1.2×10^{-7} at low dose, based on $k_T = 4\pi r_o D$. A more rigorous calculation with target theory (see section 3 of this proposal) gives $\eta_\Delta = 5 \times 10^{-8}$ corresponding to a local target on the yeast surface about 400 $\mathring{A}^2$.

Additional experiments were carried out to explore the importance of singlet oxygen as the dominant inactivating agent. The results in Fig. 22 show that the singlet oxygen quencher, N_3^-, protects against photodynamic inactivation, particularly in the high dose, exponential component. The data in Fig. 23 and Fig. 24 provide additional support, where the quantum yields are enhanced in D_2O as the medium. There is a significant temperature effect, where the high dose killing rate in D_2O was 14 times higher at 19°C and only 1.4 times higher at 30°C. The results of various experiments (Table X) indicate a temperature dependent component to photodynamic sensitivity that far exceeds the ∿25% increase in the diffusion constant of molecular oxygen in water for this temperature range.

$10^{12} \phi_i$

	t = 19°C		t = 30°C	
	low dose	high dose	low dose	high dose
$H_2O(N_2)$	0.00	0.00	0.00	0.10
$H_2O(O_2)$	0.16	0.16	0.27	1.71
$D_2O(N_2)$	0.00	0.00	0.00	0.05
$D_2O(O_2)$	0.79	4.28	0.81	3.35

Table X. Photodynamic Inactivation of Yeast Sensitized by Eosin Y

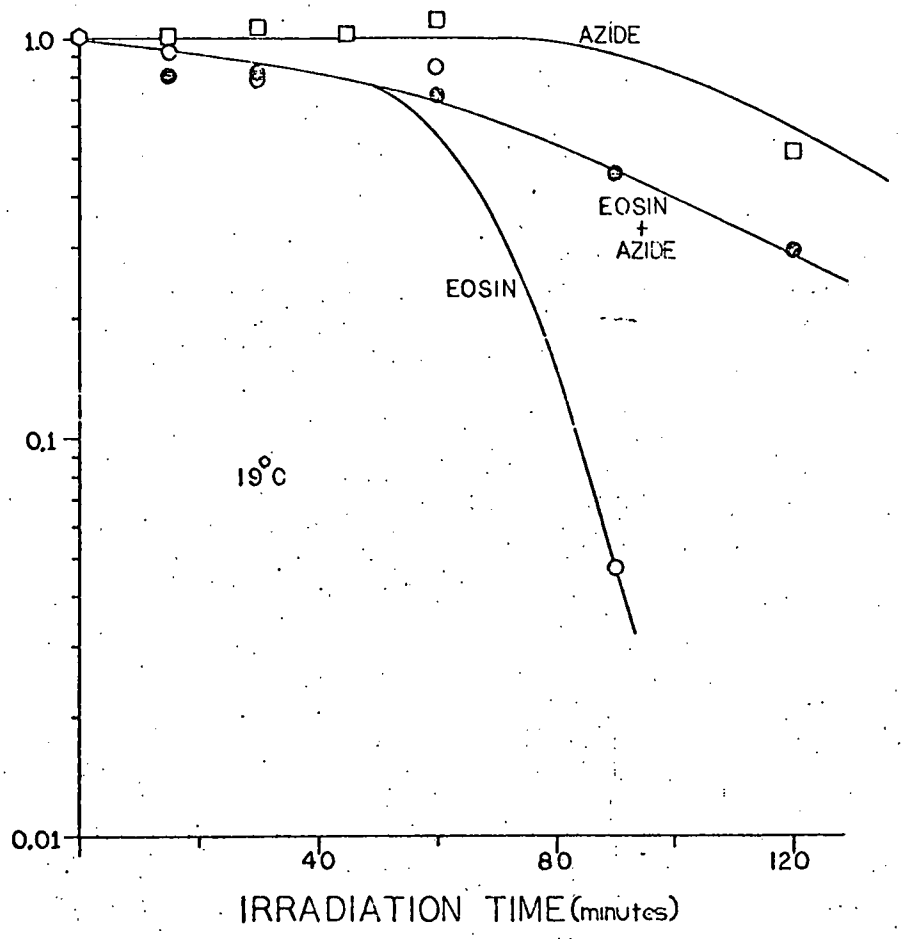

Figure 22. Photodynamic inactivation of yeast by 25 μM Eosin Y in H_2O; effect of 0.1M azide, O_2-sat

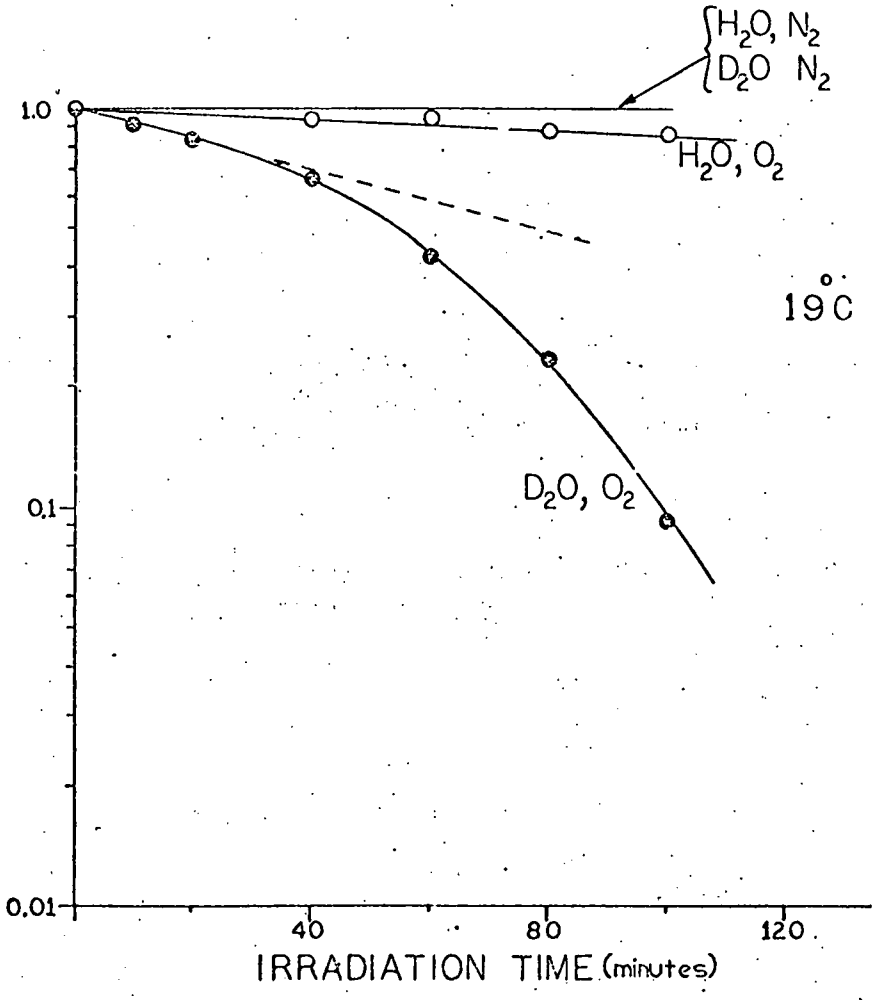

Figure 23. Photodynamic inactivation of yeast by Eosin Y; Effect of D_2O and O_2 at 19C

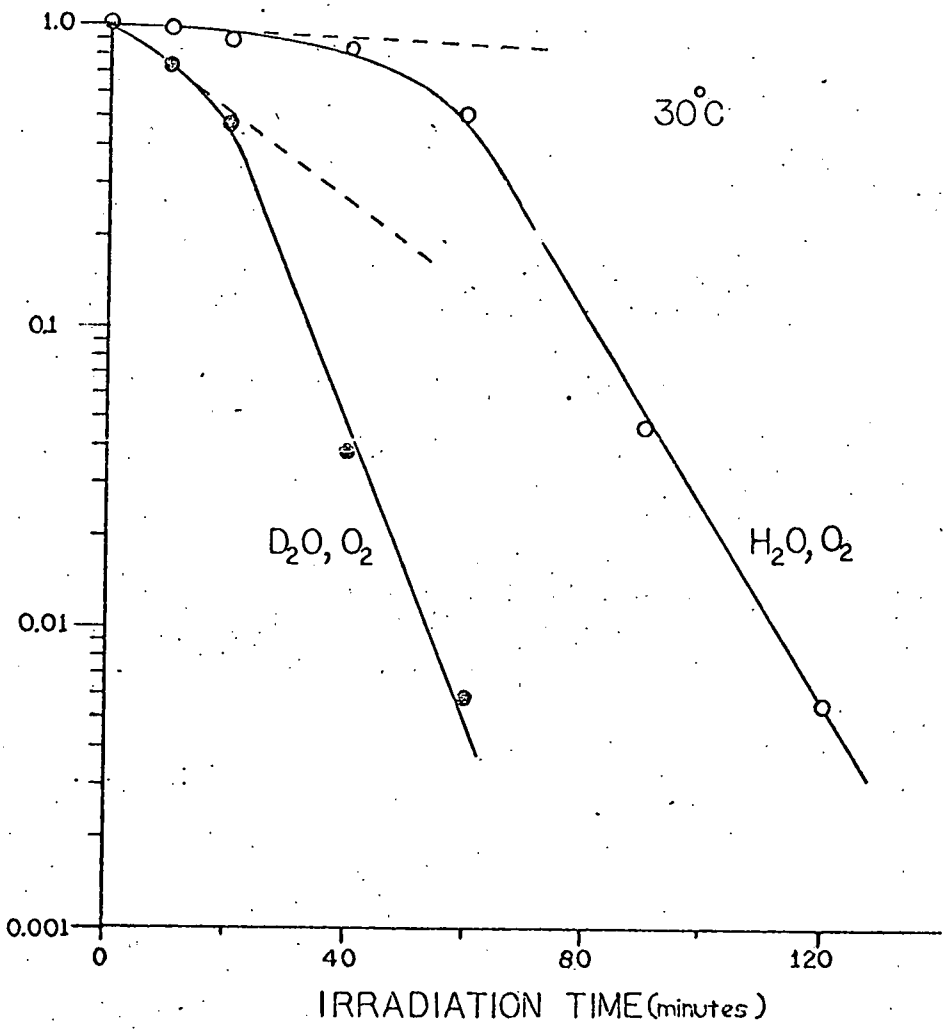

Figure 24. Photodynamic inactivation of yeast by Eosin Y; Effect of D_2O and O_2 at 30C

The sensitivity also shows a remarkable dependence on the growth stage (Fig. 25): the "plateau" stage cultures are strongly resistant, "mid-log" phase cells are high sensitive and "late-log" phase cells are equally sensitive on the high dose region but with a longer shoulder. The implications of these high dose results on the photodynamic mechanism are being explored in current spin label work.

b) Spin Label Studies of Yeast Membrane Photodynamic Damage

Nitroxide spin labels are being used as a nonperturbing probe of photodynamic damage to the yeast plasma membrane, based on the effect of the microenvironment on the motion of the probe molecule, as followed by ESR absorption measurements. Spin labeling ESR techniques have proved to be of great value in studies of the physical properties of membranes at the microscopic level under a variety of conditions (Berliner, 1976). Spin labels can be prepared by the covalent addition of a five- or six-membered ring containing a nitroxide group to a molecule which is compatible with the lipid-protein bilayer unit. Within the membrane the label assumes a position in which it samples the properties of the system (Keith et al., 1973). Rotational tumbling times of the labels can be determined from measurements of the heights and widths of the three nitroxide ESR lines (Williams et al., 1971), and these values reflect the motional hindrance caused by the rigidity of the molecular environment. Systematic variations in membrane physical properties result in corresponding changes in spin label rotational diffusion which correlate well with alterations in membrane function (Eletr et al., 1974). The hyperfine splitting between peaks and the position of the center of the spectrum both depend on the polarity of the molecular environment and can be employed to determine the partitioning of amphiphilic spin labels between aqueous and hydrocarbon regions (Hubbell and McConnell, 1968). Fluidity and order at different positions across the membrane can be investigated with the use of lipid spin labels synthesized from fatty acids or hydrocarbons in which the position of the nitroxide

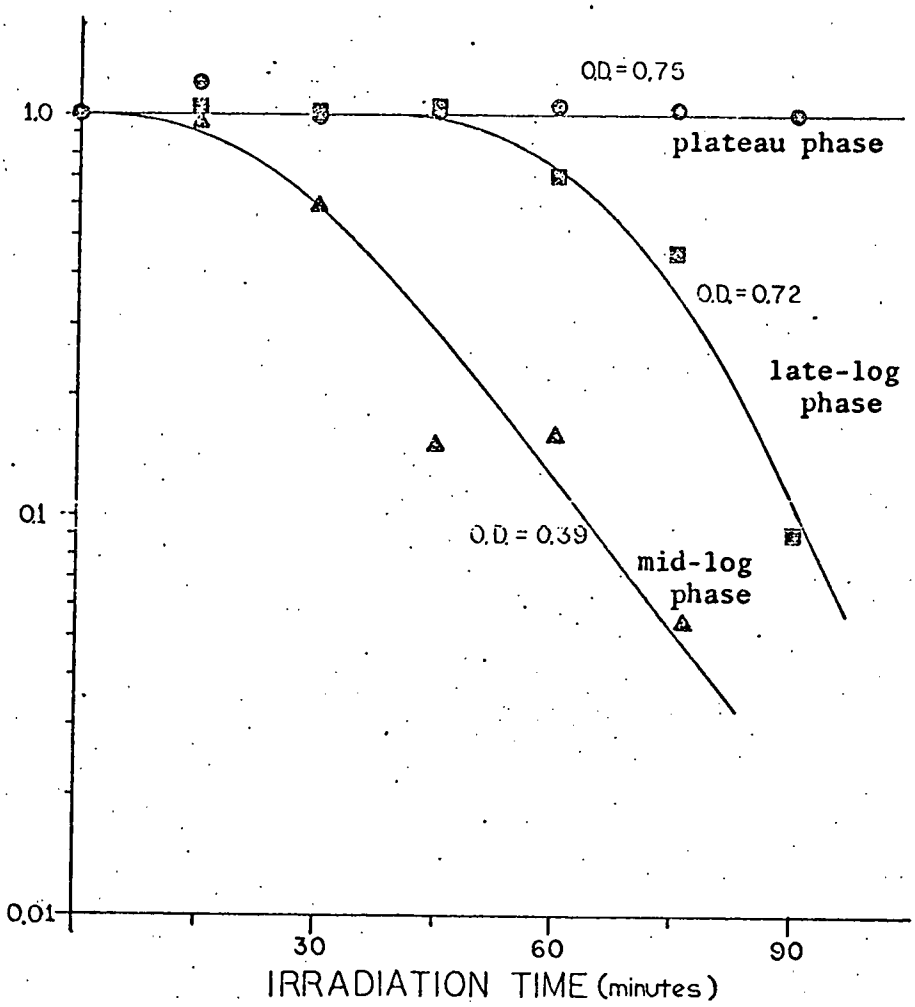

Figure 25. Photodynamic inactivation of yeast by Eosin Y; Effect of culture growth phase; O.D. = 0.75 corresponds to 10^7 cells/ml

group varies, so that a depth profile of membrane properties can be constructed (Morse et al., 1975). Accumulation of spin labels into microscopic regions of high local probe concentration within the sample can be detected by the appearance of spin exchange and magnetic dipole effects between labels (Cohn et al., 1974); Scandella et al., 1972). Each of these spectral features reflects particular microscopic physical properties of the membrane, so that a judicious choice of spin labels permits the exploration of a broad range of membrane phenomena at the molecular level.

Particular emphasis has been given in recent work to the effect of growth stage and temperature on the membrane properties. Typical spectra in Fig. 26 with lipid spin label $12NS_{me}$ (see Progress Report, 7/1/75-6/30/76) show free rotation of the spin label in the early stages of exponential growth, as evidenced by the narrow triplet spectrum. However, as the culture multiplies the spectra indicate the growth of a second contribution, corresponding to a less fluid and less polar environment which eventually dominates at the highest cell densities. The corresponding values of the rotational correlation times (Fig. 27) show that the environment of the membrane sampled by the spin label becomes more rigid as the culture passes through and past exponential growth. In similar experiments at several membrane temperatures, τ_o increases by a factor of 2 from 20°C to 30°C. These results suggest that the sensitivity of the yeast to singlet oxygen attack is inhibited by low membrane fluidity. Since only a small part of the yeast surface is sensitive to singlet oxygen, the ability of the initial lesion to propagate through the membrane may be involved in the subsequent stages of the inactivating process.

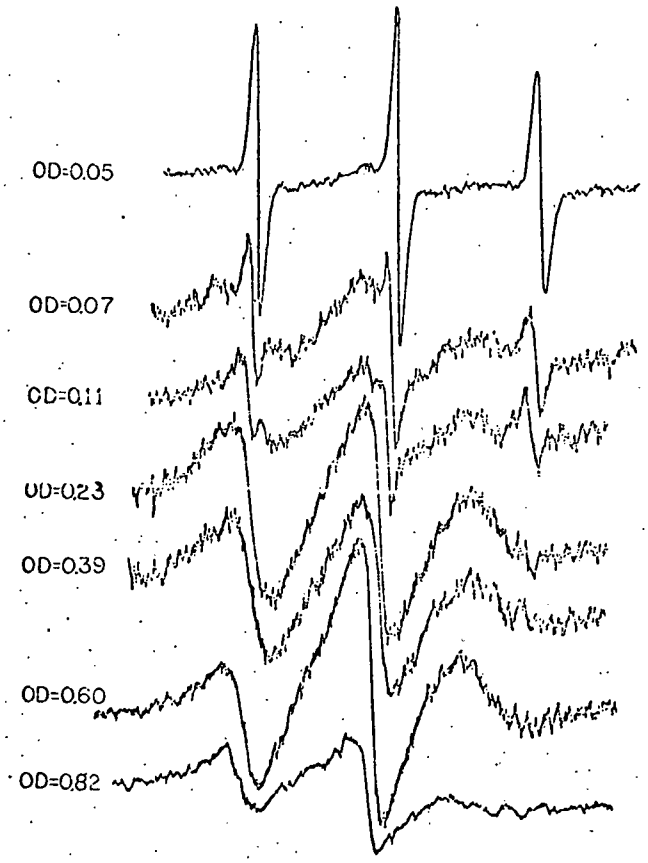

Figure 26. Effect of growth phase on ESR absorption by spin label 12NM$_{me}$ in yeast cell plasma membrane

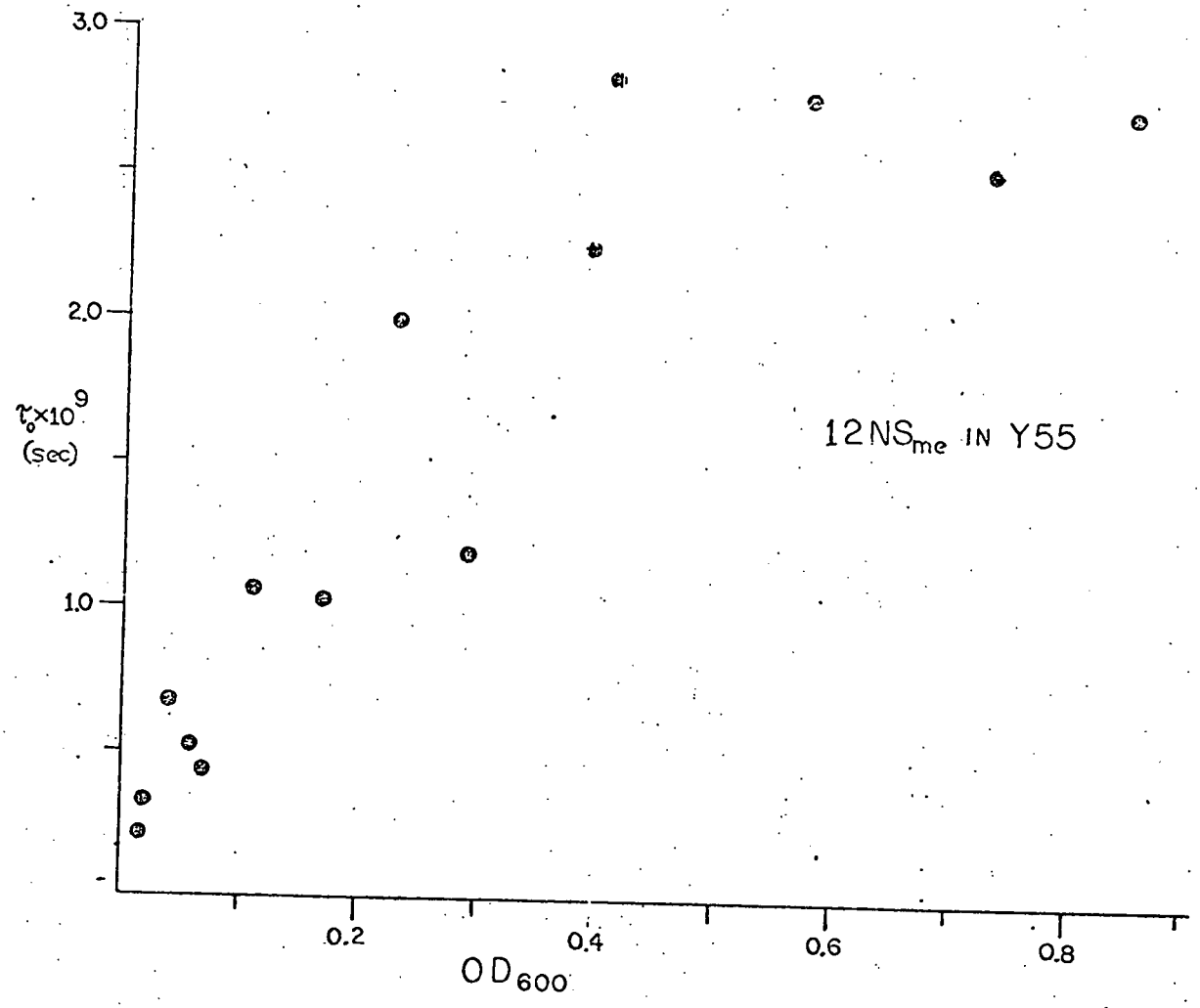

Figure 27. Effect of growth phase on rotational correlation time of spin label 12NS$_{me}$ in yeast cell plasma membrane

LITERATURE REFERENCES

Alexander, P. and Lett, J.T. (1960). Nature 187, 933.

Baugher, J.F. and Grossweiner, L.I. (1977). J. Phys. Chem., in press.

Becker, D., Grossweiner, L.I., Ovadia, J. and Redpath, J.L. (1975). Int. J. Radiat. Biol. 28, 195.

Becker, D., Redpath, J.L. and Grossweiner, L.I. (1977). Radiat. Res., in press.

Bevilacqua, R. and Bordin, F. (1973). Photochem. Photobiol. 17, 191.

Blok, J. and Loman, H. (1973). Current Topics in Radiation Research Quarterly (M. Ebert and A. Howard, Eds.). Vol. 9, North-Holland Publishing Co., Amsterdam, pp. 165-245.

Bryant, F.D., Santus, R. and Grossweiner, L.I. (1975). J. Phys. Chem. 79, 2711.

Cohn, G.E., Keith, A.D. and Snipes, W.C. (1974). Biophys. J. 14, 178.

Cohn, G.E., Tien, A.F. and Grossweiner, L.I. (1977). Bull. Am. Phys. Soc. 22, 42.

Cohn, G.E. and Tseng, H.Y. (1977). Photochem. Photobiol., in press.

Dainton, F.S. and Logan, S.R. (1965). Proc. Roy. Soc. London, A287, 281.

Gervais, J. and Schryver, F.C.D. (1975). Photochem. Photobiol. 21, 71.

Glad, B.W. and Spikes, J.D. (1966). Radiation Res. 27, 237.

Grossweiner, L.I. (1976). In Current Topics in Radiation Research Quarterly, (M. Ebert and A. Howards, Eds.). Vol. 11, North-Holland Publishing Co., Amsterdam, pp. 141-199.

Grossweiner, L.I., Kaluskar, A.G. and Baugher, J.F. (1976). Int. J. Radiat. Biol. 29, 1.

Grossweiner, L.I. and Baugher, J.F. (1977). J. Phys. Chem. 81, 93.

Grossweiner, L.I. (1977). Photochem. Photobiol., in press.

Hagen, U. and Wellstein, H. (1965). Strahlentherapie 128, 565.

Hawkins, R.B. (1976). Radiat. Res. 63, 300.

Hutchinson, F. (1957). Radiat. Res. 7, 473.

Imamura, M. (1956). J. Inst. Polytech. 5, 85.

Imoto, T., Forster, L.S., Rupley, J.A. and Tanaka, F. (1971). Proc. Natn. Acad. Sci. U.S.A., 69, 1151.

Ito, T. and Kobayashi, K. (1974). Sci. Papers Coll. Gen. Ed. (University of Tokyo) 24, 33.

Jagger, J. (1967). Introduction to Research in Ultraviolet Photobiology, Prentice Hall, Englewood Cliffs, New Jersey, pp. 60-76.

Jortner, J., Ottolenghi, M. and Stein, G. (1962a). J. Phys. Chem. 66, 2029.

Jortner, J., Ottolenghi, M. and Stein, G. (1962b). J. Phys. Chem. 66, 2037.

Jortner, J., Ottolenghi, M. and Stein, G. (1962c). J. Phys. Chem. 66, 2042.

Jortner, J., Ottolenghi, M. and Stein, G. (1962d). J. Phys. Chem. 37, 2488.

Jortner, J., Ottolenghi, and Stein, G. (1963). J. Am. Chem. Soc. 85, 2712.

Jortner, J., Ottolenghi, M. and Stein, G. (1964). J. Phys. Chem. 68, 247.

Kepka, A.G. and Grossweiner, L.I. (1973). Photochem. Photobiol. 18, 49.

Land, E.J. (1977). American Society for Photobiology, May 11-15, 1977, San Juan.

Mantulin, W.W. and Song, P.S. (1973). J. Am. Chem. Soc. 95, 5122.

Matheson, I.B.C., Etheridge, R.D, Kratowich, R. and Lee, J. (1975). Photochem. Photobiol. 21, 165.

McCormick, J.P., Fischer, J.R., Pachlatko, J.P. and Eisenstark, A. (1976). Science 191, 468.

Michelson, A.M. and Durosay, P. (1977). Photochem. Photobiol. 25, 55.

Moore, T.A., Montgomery, A.B. and Kwiram, A.L. (1976). Photochem. Photobiol. 24, 83.

Morowitz, H.J. (1950). Science 111, 229.

Morse, P.D., II, Ruhlig,, M., Snipes, W. and Keith, A.D. (1975). Arch. Biochem. Biophys. 168, 40.

Musajo, L. and Rodighiero, G. (1972). In Photophysiology, (A.C. Giese, Ed.), Vol. VII, Academic Press, New York, pp. 115-147.

Musajo, L., Rodighiero, G., Caporale, G., Dall'Acqua, F., Marciani, S., Bordin, F., Baccichetti, F. and Bevilacqua, R. (1974). Sunlight and Man (T.B. Fitzpatrick, Ed.) University of Tokyo Press, Tokyo, pp. 335-368.

Myers, L.S., Jr., Hollis, M.L. and Theard, L.M. (1968). Advances in Chemistry Series 81 (R.F. Could, Ed.), American Chemical Society, Washington, D.C., pp. 345-367.

Noyes, R.M. (1955). J. Am. Chem. Soc. 77, 2042.

Noyes, R.M. (1956). J. Am. Chem. Soc. 78, 5486.

Noyes, R.M. (1961). Progress in Reaction Kinetics (G. Porter, Ed.), Pergamon Press, New York, p. 129.

Pathak, M.A., Allen, B., Ingram, D.J.E. and Fellman, J.H. (1961). Biochim. Biophys. Acta. 54, 506.

Pathak, M.A., Kramer, D.M. and Fitzpatrick, T.B. (1974). Sunlight and Man (T.B. Fitzpatrick, Ed.), University of Tokyo Press, Tokyo, pp. 335-368.

Poppe, W. and Grossweiner, L.I. (1975). Photochem. Photobiol. 22, 217.

Roberts, P.B. (1973). Int. J. Radiat. Biol. 24, 143.

Scandella, C.J., Devaux, P. and McConnell, H.M. (1972). Proc. Natl. Acad. Sci. U.S.A. 69, 2056.

Song, P.S., Harter, M.L. and Herndon, W.C. (1971). Photochem. Photobiol. 14, 521.

Usui, Y., Itoh, K. and Koizumi, M. (1965). Bull. Chem. Soc. Japan 18, 1015.

Usui, Y. (1973). Chemistry Letters (Japan), 743.

Van der Schans, G.P., Bleichrodt, J.F. and Blok, J. (1973). Int. J. Radiat. Biol. 23, 133.

Van der Schans, G.P. and Bleichrodt, J.F. (1974). Int. J. Radiat. Biol. 26, 121.

Walrant, P., Santus, R. and Grossweiner, L.I. (1975). Photochem.Photobiol. 22, 163.

Zigman, S., Hare, J.D., Yulo, T. and Ennist, D. (1977). American Society for Photobiology, May 11-15, 1977, San Juan.

REPORTING OF RESEARCH*

A. Journal Articles

1. "Photochemical Inactivation of Enzymes" (Review Article)
   L.I. Grossweiner
   CURRENT TOPICS IN RADIATION RESEARCH QUARTERLY,
   Vol. 11, North-Holland, Amsterdam, 1976, pp. 141-199. COO-2217-14

2. "Flash Photolysis of Enzymes"
   L.I. Grossweiner, A.G. Kaluskar and J.F. Baugher
   INT.J.RADIAT.BIOL. 29, 1-16 (1976). COO-2217-9

3. "Decay Kinetics of the Photochemical Hydrated Electron"
   L.I. Grossweiner and J.F. Baugher
   J.PHYS.CHEM. 81, 93-98 (1977) COO-2217-17

4. "Laser Flash Photolysis of Lysozyme"
   J.F. Baugher, L.I. Grossweiner, and J.Y. Lee
   PHOTOCHEM.PHOTOBIOL. 25, 305-306 (1977) COO-2217-19

5. "Photolysis Mechanism of Aqueous Tryptophan"
   J.F. Baugher and L.I. Grossweiner
   J.PHYS.CHEM. (in press) COO-2217-18

6. "Photodynamic Inactivation of Yeast Sensitized by Eosin Y"
   G.E. Cohn and H.Y. Tseng
   PHOTOCHEM.PHOTOBIOL. (in press) COO-2217-20

B. Meetings

1. Radiation Research Society, San Francisco, June 27-July2, 1976
   "Laser Flash Photolysis of Enzymes"
   J.F. Baugher and L.I. Grossweiner

2. American Physical Society, Chicago, February 7-10, 1977
   a) "Photoionization of Tyrosyl Peptides in Aqueous Solution"
      J.F. Baugher and L.I. Grossweiner
   b) "$^1O_2$* Mechansim of Eosin-Sensitized Photodynamic Inactivation of Saccharomyces cerevisiae"
      G.E. Cohn, A.F. Tien and L.I. Grossweiner

3. American Physical Society, San Diego, March 21-24, 1977
   "Recombination Kinetics of Photoelectrons in Aqueous Media" (Invited)
   L.I. Grossweiner

4. American Society for Photobiology, San Juan, May 11-15, 1977
   a) "Photolysis Mechanism of Aqueous Tryptophan"
      J.F. Baugher and L.I. Grossweiner
   b) "Non-Homogeneous Decay Kinetics of the Photochemical Hydrated Electron"
      L.I. Grossweiner and J.F. Baugher

Project Activity

The expenditure of scientific effort and funds was consistent with the technical program in the Renewal Proposal and the current budget.

Scientific Salaries

Dr. Leonard I. Grossweiner (Professor): 10% of time 1976-77 academic year; 1 month Summer 1977

Dr. Joseph F. Baugher (Assistant Professor): 1 month Summer 1976

Dr. Gerald E. Cohn (Assistant Professor): 1 month Summer 1976; 10% of time 1976-77 academic year; 1 month Summer 1977

Dr. Joon Lee (Research Associate): 100% of time 7/1/76-9/30/77

Foreign Travel

none

Non-Salaried Student Participants

Mr. Eric Zickgraf: Graduate Teaching Assistant, 1976-77 academic year